Ecological Indicators 150 (2023) 110271

Contents lists available at ScienceDirect

Ecological Indicators

journal homepage: www.elsevier.com/locate/ecolind

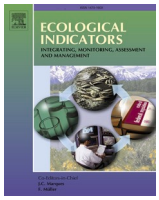

Soil moisture content-based analysis of terrestrial ecosystems in China: Water use efficiency of vegetation systems

Hao Ding [a,b,c], Zhe Yuan [b,c,*], Xiaoliang Shi [a,*], Jun Yin [d], Fei Chen [a], Mengqi Shi [a,b,c], Fulong Zhang [e]

[a] College of Geomatics, Xi'an University of Science and Technology, Xi'an 710054, China
[b] Changjiang River Scientific Research Institute, Changjiang Water Resources Commission of the Ministry of Water Resources of China, Wuhan 430010, China
[c] Hubei Key Laboratory of Water Resources & Eco-Environmental Sciences, Wuhan 430010, China
[d] Department of Geographical Sciences, Faculty of Resources and Environmental Science, Hubei University, Wuhan 430062, China
[e] Xi'an Medical University, Xi'an 710054, China

ARTICLE INFO

Keywords:
Soil moisture use efficiency
Precipitation use efficiency
Relative contribution
Climate factor
China

ABSTRACT

Water is a prerequisite for the formation of earth-biochemical-ecological systems. Differences in the spatial and temporal distribution of water resources are important factors in the formation of differences in the distribution of vegetation in terrestrial ecosystems and are key to the differences in vegetation productivity. Vegetation water use efficiency is calculated by the total amount of fixed biogenic carbon per unit mass of water consumed in photosynthesis and can be used to assess the intensity and capacity of an ecosystem to use water biomass. Based on remote satellite sensing data, this study proposes a new water use efficiency assessment model. The model was validated using flux site data, and we analyzed the relative contribution of climate factors to soil moisture use efficiency using a first-difference method. The results revealed the following: (1) The soil moisture use efficiencies (SUE) of remote sensing data inversions that were evaluated using flux site data based on correlation coefficients and Nash coefficients showed high reliability, and only the NMG (Inner Mongolia) station showed low correlation among the nine sites. (2) Among the nine agricultural sub-regions in China, only the SUE of the Qinghai-Tibet Plateau region showed a decreasing trend (-1.08 g C/m^{-2} kg H_2O yr), while all other regions showed an increasing trend. (3) The highest vegetation soil moisture use efficiency (1.83 g C/m^{-2} kg H_2O) was found in ferralisols, while the lowest vegetation SUE (0.17 g C/m^{-2} kg H_2O) was found in arid soils. The SUE of different vegetation types showed the characteristics of forest > scrub > cultivated vegetation > wetland > grassland. (4) The relative contribution of gross primary productivity (GPP) to the change in SUE was 37.53%, while the relative contribution of soil moisture content to the change in SUE was −26.71%. Among the five climatic factors, temperature was the most dominant factor affecting the change in SUE, followed by precipitation, net radiation, leaf area index, and potential evapotranspiration. Revealing the relationship between terrestrial ecosystem GPP, soil moisture content, and their responses to climate factors is a prerequisite for understanding the adaptation strategies of regional terrestrial ecosystems to global climate change, which can help to inform decision-making for the sustainable development of ecosystems.

1. Introduction

The concentration of greenhouse gases in the atmosphere has continued to increase over recent decades (Zhang et al., 2020), leading to global warming, reduced precipitation, and increased evaporation from the Earth's surface, conferring profound effects on the stability of terrestrial ecosystems (Qin et al., 2020). To effectively respond to climate change, it is important to understand how climate change affects the biochemical mechanisms of terrestrial vegetation (Tougeron et al., 2020; Xia et al., 2020), especially the carbon and water cycles that maintain the balance and stability of terrestrial ecosystems (Heimann and Reichstein, 2008; Li et al., 2021; Li et al., 2020). Water use efficiency is an important physiological variable of vegetation and a key indicator of the relationship between water consumption and vegetation

* Corresponding authors at: Changjiang River Scientific Research Institute, Changjiang Water Resources Commission of the Ministry of Water Resources of China, Wuhan 430010, China (Z. Yuan); College of Geomatics, Xi'an University of Science and Technology, Xi'an 710054, China(X. Shi)
E-mail addresses: yuanzhe_0116@126.com (Z. Yuan), xiaoliangshi@xust.edu.cn (X. Shi).

https://doi.org/10.1016/j.ecolind.2023.110271
Received 8 February 2023; Received in revised form 13 April 2023; Accepted 16 April 2023
Available online 23 April 2023

as a carbon sink (An, 2022). Vegetation water use efficiency has become a hot topic in the study of the carbon and water cycles of ecosystems. Thus, it is important to analyze the changing characteristics of water use efficiency of vegetation and its influencing factors (Zhang et al., 2016), not only to grasp the characteristics of the carbon and water cycles of ecosystems in the context of climate change but also to understand the response relationship of terrestrial ecosystems to climate change (Hatfield and Dold, 2019), which is significant for the sustainable development of ecosystems.

Vegetation water use efficiency is a key indicator of ecosystem and a core element of ecosystem water cycle, carbon cycle and energy cycle. In different application scenarios, water use efficiency has different physical meanings. From the perspective of crop yield, water use efficiency is defined as the amount of carbon sequestered per unit of transpiration or crop yield. From the perspective of the water supply side, it is defined as the ratio of evapotranspiration of irrigation water to the total water supply (Sun et al., 2020; Wang et al., 2023). Vegetation water use efficiency includes water use efficiency (WUE) and precipitation use efficiency (PUE), where WUE is defined as the ratio of gross primary productivity (GPP) to evapotranspiration, and PUE is defined as the ratio of GPP to precipitation (Gu et al., 2021; Liu et al., 2022) and integrates the relationship between the characteristics of carbon sequestration and water consumption (de Oliveira et al., 2018). Scientists have conducted studies on vegetation water use efficiency at different spatial and temporal scales for typical global regions. However, previous studies have overlooked an important issue: precipitation is an important source of surface water recharge, but it is not directly used by vegetation (LucLambs, 2004). Precipitation is converted to soil moisture through infiltration before it can be absorbed by vegetation roots (Mei and Ma, 2022). Vegetation water use efficiency has been evaluated globally at the individual and ecosystem scales using methods such as tree annual cycle carbon isotopes, eddy flux measurements, atmospheric carbon isotope composition analysis, and Earth system modeling techniques (Guerrieri et al., 2019; Van der Sleen et al., 2015). However, relevant research has shown that a reduction in soil moisture reduces the vegetation activity and slows photosynthetic efficiency; therefore, it is necessary to analyze vegetation WUE based on soil moisture.

Soil moisture content is influenced by precipitation, soil type, soil characteristics, vegetation status, and human activities (Fenger-Nielsen et al., 2019). Previous related studies have analyzed the response of vegetation WUE to variables such as climate factors, land cover change, and different vegetation types (Gao et al., 2014; Nandy et al., 2022; Song et al., 2017; Zhu et al., 2011). However, little research has been conducted into the characteristics of vegetation and how WUE changes in different soil types. There are great differences in soil properties between different types of soils, and China has a wide variety of soil types, and their spatial distribution varies significantly (Fu et al., 2018). For example, in the Loess Plateau region of China, the soil type is mainly primary soil. This type of soil is mostly distributed in areas with sparse vegetation and severe soil erosion. Hou et al. (2022) found that there were significant seasonal differences in vegetation WUE on the Loess Plateau (summer > autumn > spring). In the Qinghai-Tibet Plateau region of China, the soil type is dominated by alpine soils. The most important characteristic of alpine soils compared with other types of soil is that they have a seasonal freezing layer or permafrost phenomenon. Ji et al. (2022) found that vegetation WUE in the Qinghai-Tibet Plateau region was on the rise, and that temperature was the dominant factor affecting vegetation WUE. In previous regional studies, however, the differences in WUE between different soil types were not well explained.

With the development of remote sensing technology in recent years, a new way to study ecosystem carbon cycles and water cycles on a large scale has been provided (Xiao et al., 2019). However, compared with flux site data, there are disadvantages, including lower spatial resolution. Therefore, data from nine carbon flux observation sites in the Chinese region based on the eddy covariance technique were used in this study to validate the vegetation SUE based on the inversion of remote sensing data. The combination of remote sensing data and flux data was used to analyze the differences in the spatial and temporal distribution of vegetation WUE in China and the sensitivity to climatic and environmental factors.

Over the past few decades, ecological projects implemented by the Chinese government have made significant contributions to the increase in global carbon sinks (Fang et al., 2018). However, due to the impact of global warming, the changing characteristics of vegetation WUE in China still deserve to be studied and will provide a reference for the study of vegetation carbon and water cycles in other regions of the world (Zhong et al., 2021). Based on this, the objectives of this study were to: (1) analyze the changes in SUE in nine agricultural sub-regions of China; (2) compare the differences in SUE of vegetation between different soil types and vegetation types; (3) conduct attribution analysis of the changes in vegetation SUE based on multiple climatic factors; (4) analyze the spatial and temporal differences between vegetation precipitation use efficiency and SUE.

2. Data and methods

2.1. Data sources

2.1.1. Soil moisture content data

The soil moisture dataset was obtained from the data center of the Ecological Discipline of the Chinese Academy of Sciences (https://www.nesdc.org.cn). The data was based on the downscaling technique of spatial weighting of MODIS/TVDI data, using soil moisture data from different passive microwave products, including AMSR-E and AMSR2 JAXA Level 3 products, and AMOS-IC data products, obtained after calibration and reconstruction with ground monitoring data using a unified model (Meng et al., 2021). The soil moisture dataset has a spatial resolution of 0.05° and a temporal resolution of months and is widely used in hydrological and drought monitoring studies.

2.1.2. Remote sensing data

Satellite-based solar-induced chlorophyll fluorescence (SIF) has proven to be remarkably promising for monitoring terrestrial photosynthesis. Based on the finer resolution SIF product derived from the Orbiting Carbon Observatory 2 (OCO-2) (GOSIF), the GOSIF GPP dataset was generated by using the strong linear relationships between the tower GPP data and the GOSIF data (Li and Xiao, 2019). The monthly GOSIF GPP data, with a spatial resolution of 0.05° during the period of 2000–2018, was used in this study.

2.1.3. Climate data

The climate data used in this study included precipitation, temperature, evapotranspiration, net radiation (RN), and the monthly leaf area index (LAI) data sourced from the National Tibetan Plateau Scientific Data Center (https://data.tpdc.ac.cn/), with a spatial resolution of 1 km (Chen et al., 2021). The above climate data are synthesized on an annual scale according to the corresponding laws.

2.1.4. Flux site data

The flux site dataset used in this study was sourced from the Ecological Discipline Data Center of the Chinese Academy of Sciences (https://www.nesdc.org.cn). The flux data from 2004 to 2010 were selected from nine sites in Xishuangbanna, Changbai Mountain, Dinghu Mountain, Dangxiong, Haibei scrub, Haibei wetland, Inner Mongolia, Qianyanzhou, and Yucheng (Yu et al., 2014). The data products used were monthly values of flux data, including net ecosystem exchange (NEE), gross ecosystem exchange, ecosystem respiration, sensible heat, and latent heat, after standardized quality control and data processing using the China Flux technical system.

2.1.5. Agricultural zoning, soil type, and vegetation type data

The topography of China is high in the west and low in the east, with

mountains, plateaus, and hills accounting for 67% of the total land area and basins and plains accounting for 33% of the total land area. Due to the significant differences in terrain height and diverse topography in China, the climatic environment is complex and variable. Based on this, the nine agricultural zones of China provided by the Resource and Environmental Science and Data Center (https://www.resdc.cn) were used to delineate the study area in this paper. This zoning approach fully considered the similarity of regional natural climatic characteristics, the degree of economic development, and crop types. The area names and their spatial locations are shown in Fig. 1.

Soil and vegetation type data were provided by the Resource and Environmental Science and Data Center of the Chinese Academy of Sciences (https://www.resdc.cn), and the spatial resolution of the soil and vegetation type data was 1,000 m. The soil types included 12 soil classes and 61 soil types, and the vegetation types included 13 major vegetation classes and 58 subclasses. In this study, all of them were analyzed according to the major soil and vegetation classes. Details of the datasets used in this study for drought indexing are provided in Table 1.

Table 1
The datasets used in this study.

Data	Spatial resolution	Temporal resolution	Time span	Link
GPP data	0.05°	monthly/ yearly	2002–2018	https://global ecology.unh.edu
Soil moisture content data	0.05°	monthly	2002–2018	https://www.nes dc.org.cn
Climate data	1 km	monthly	2002–2018	https://data.tp dc.ac.cn/
Flux site dataset		yearly	2004–2010	https://www.nes dc.org.cn
Soil and vegetation type data	1 km	yearly	2015	https://www. resdc.cn

2.2. Methods

2.2.1. Site-scale GPP calculation

GPP can be obtained using the ecosystem respiration (RE) and NEE, calculated from CO_2 flux observations, as in Eq. (1):

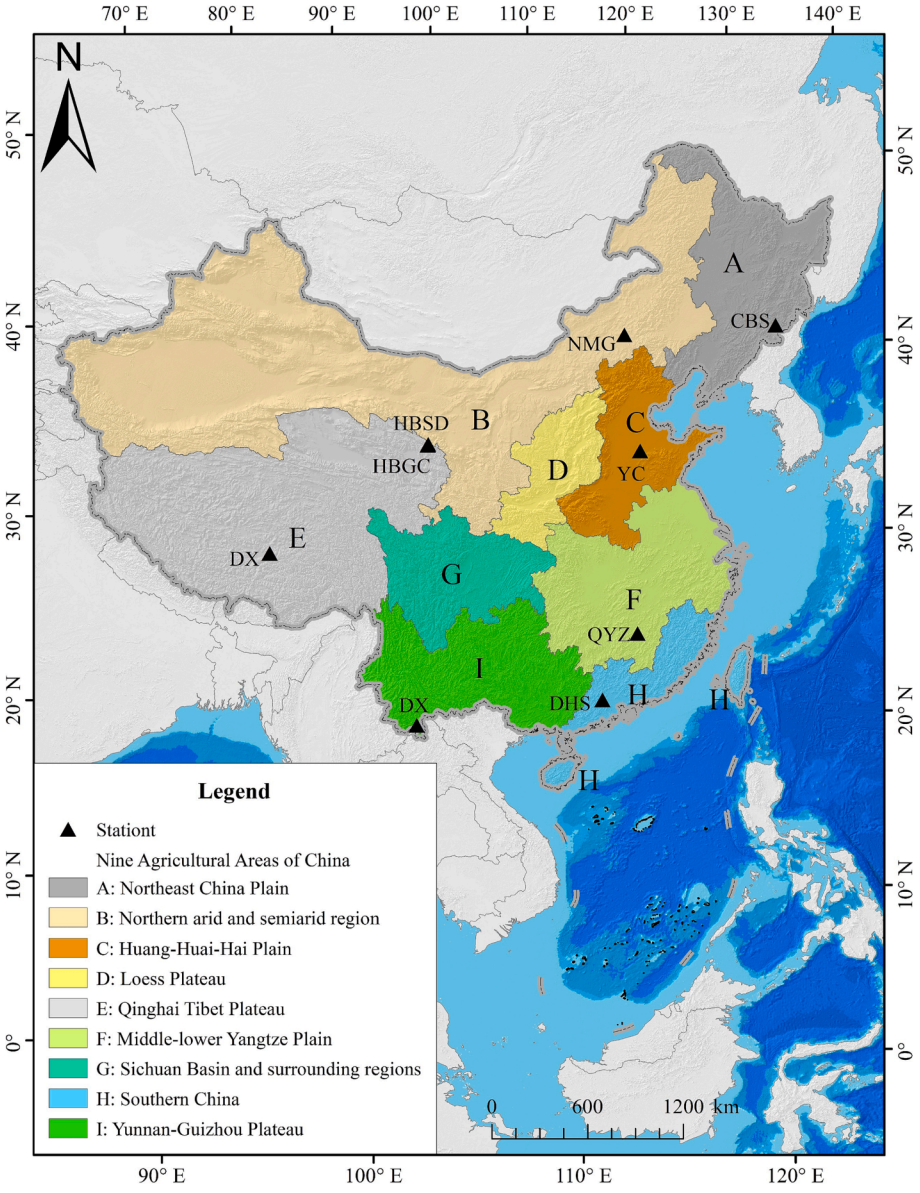

Fig. 1. Spatial distribution of agricultural divisions and flux sites.

$$GPP = RE - NEE \quad (1)$$

Ecosystem respiration includes autotrophic respiration (vegetation respiration) and heterotrophic respiration (soil respiration). Both RE and NEE can be calculated from turbulent fluxes of CO_2 and storage fluxes of CO_2 at measured altitudes (Li et al., 2016).

2.2.2. Vegetation WUE

In this study, two vegetation water use efficiencies were calculated: precipitation use efficiency (PUE) and soil moisture use efficiency (SUE), where PUE was defined as the ratio of GPP to precipitation, and SUE was defined as the ratio of GPP to soil moisture content (Liu et al., 2022) (Eq. (2)).

$$SUE = GPP/_{SM} \quad (2)$$

$$PUE = GPP/_{PRE} \quad (3)$$

where GPP represents the monthly or annual gross primary productivity of vegetation (g C/m^2), soil moisture (SM) represents the moisture per cubic meter of soil (m^3/m^3), and PRE represents the monthly or annual precipitation (mm). (The gray areas are used in the full text to indicate SUE and PUE as missing data.)

2.2.3. SUE validation method

In this study, the Pearson correlation coefficient and the Nash–Sutcliffe coefficient were used to verify the SUE based on the inversion of remote sensing data. The Pearson correlation coefficient reflects the linear relationship between two sets of variables; the closer the Pearson correlation coefficient is to 1, the stronger the linear relationship between the variables. The Nash–Sutcliffe coefficient is mostly applied to verify the merit of the results of a hydrological model simulation; the closer the Nash–Sutcliffe efficiency (NSE) is to 1, the more credible the model. The Pearson correlation coefficient and Nash–Sutcliffe coefficient are calculated as follows:

$$R = \frac{1}{n-1}\sum_{t=1}^{n}\left(\frac{X_t - \overline{X}}{\sigma_X}\right)\left(\frac{Y_t - \overline{Y}}{\sigma_Y}\right) \quad (4)$$

$$NSE = 1 - \frac{\sum_{t=1}^{n}(X_t - Y_t)^2}{\sum_{t=1}^{n}(X_t - \overline{X})^2} \quad (5)$$

where X represents the vegetation SUE from flux site inversion, Y represents the vegetation SUE from remote sensing data inversion, and t is the time scale (Jan 2004 to Dec 2010).

2.2.4. Attribution analysis of changes in SUE

To quantify the influence of each climate factor on SUE, GPP, and soil moisture content, a first- difference analysis was used to quantify the relative contribution of each (Liu et al., 2018). First, a linear regression model with year as the independent variable was constructed to calculate the trends of SUE, GPP, soil moisture content, and major climate factors, including precipitation, temperature, potential evapotranspiration, LAI, and effective surface radiation over the study years, calculated as follows:

$$S_x = \frac{\partial X}{\partial T}Year + B_x \quad (6)$$

where S_x represents the values of SUE, GPP, soil moisture content, and climate factors at the corresponding stage, *Year* represents the year, B_x represents the intercept of the regression model, and $\frac{\partial X}{\partial T}$ represents the slope of the regression model, i.e., the trend of change, reflecting the characteristics of the variables as the year increases, and the slope of the regression model for SUE, GPP, and soil moisture content reflects the combined effect of climate change on their changes.

The first-difference method is a common de-trending analysis method used to establish the relationship between climate factors and ecological indicators, which can effectively reduce the influence of the remaining non-normal factors on the long-term trend of ecological indicators. The first-difference is the absolute difference ($\Delta Y = Y_{t+1} - Y_t$) for two consecutive years, and the calculated results are applied to construct a regression model to estimate the response of ecological indicators to the main climate factors. The constructed multiple regression model is shown below.

$$\Delta Y\left(SUE \quad or \quad GPP \quad or \quad SM\right) = \sum_{i=1}^{n}(S_{x_i} \bullet \Delta X_i + B_{x_i}) \quad (7)$$

where ΔY and ΔX_i are the first-differences in the corresponding time periods,B_{x_i} represents the intercept of the regression model, and S_{x_i} represents the sensitivity of the climate factors to ecological indicators.

The relative contributions of the main climatic factors to SUE, GPP, and soil moisture content were calculated as follows:

$$RC_{x_i} = \frac{S_{x_i} \bullet \frac{\partial X_i}{\partial T}}{\sum_{i=1}^{n}\left(\left|S_{x_i} \bullet \frac{\partial X_i}{\partial T}\right|\right)} \quad (8)$$

3. Results

3.1. Validation of SUE results

The results of the correlation coefficients between the SUE based on the inversion of remote sensing data and the vegetation SUE based on the inversion of site flux data are shown in Table 2. Among the nine stations, except for the Inner Mongolia station, the correlation coefficients between SUERS and SUEST were greater than 0.75, and all of them passed the 99% significance test. The moderate correlation stations included Dangxiong station and Dinghu station; the high correlation stations included Qianyanzhou station; and the significant correlation stations included Changbaishan station, Haibei wetland station, Haibei irrigation bush station, Yucheng station, and Xishuangbanna station. Except for the Inner Mongolia station, the NSEs of all stations were greater than zero, and the NSE of the Inner Mongolia station was close to 0, indicating that the SUE results from the inversion of remote sensing data were close to the average of the station results. Overall, the SUE based on the inversion of remote sensing data had high confidence and can be applied to the monitoring of vegetation WUE on a large scale.

3.2. Trends of SUE, GPP, and soil moisture (SM)

The trends of GPP, SM, and SUE in each division from 2003 to 2018 are shown in Fig. 2. The trends of GPP, SM, and SUE in different sub-regions showed obvious differences. The GPP in all sub-regions maintained the trend of growth, and the higher growth rate included Regions H, I, D, and F. Soil moisture content also showed the trend of growth in all regions except Regions B, F, and H, among which the growth rate was higher in Regions A, C, and E, while other regions maintained a relatively stable state. SUE maintained the trend of growth in all regions (except Region E), among which the growth rate was higher in Regions F and H. With the exception of Region E, all regions maintained an increasing trend, among which, Regions F and H had the highest growth rates.

Comparing the trends of GPP, SM, and SUE, it was found that the degree of influence of GPP and SM on SUE varied greatly in different sub-regions. The area north of Qinling and Huaihe River is an important climate divider in China. The area north of Qinling and the Huaihe River, including Regions A, B, C, and D, is dry, with little rain and four distinct seasons. The area south of Qinling and the Huaihe River, including Regions F, G, H, and I, has a humid climate and abundant precipitation. Region E includes the Qinghai-Tibet Plateau region, which has its own unique climate characteristics. From the trend of soil

Table 2
Comparison of inversion SUE results based on remote sensing data and site data.

Station	CBS	NMG	HBSD	HBGC	YC	DX	DHS	QYZ	XSBN
R	0.949**	0.205	0.924**	0.909**	0.962**	0.795**	0.771**	0.864**	0.938**
NSE	0.877	−0.051	0.591	0.533	0.487	0.539	0.782	0.437	0.669

Note: ** represents passing the 99% significance test.

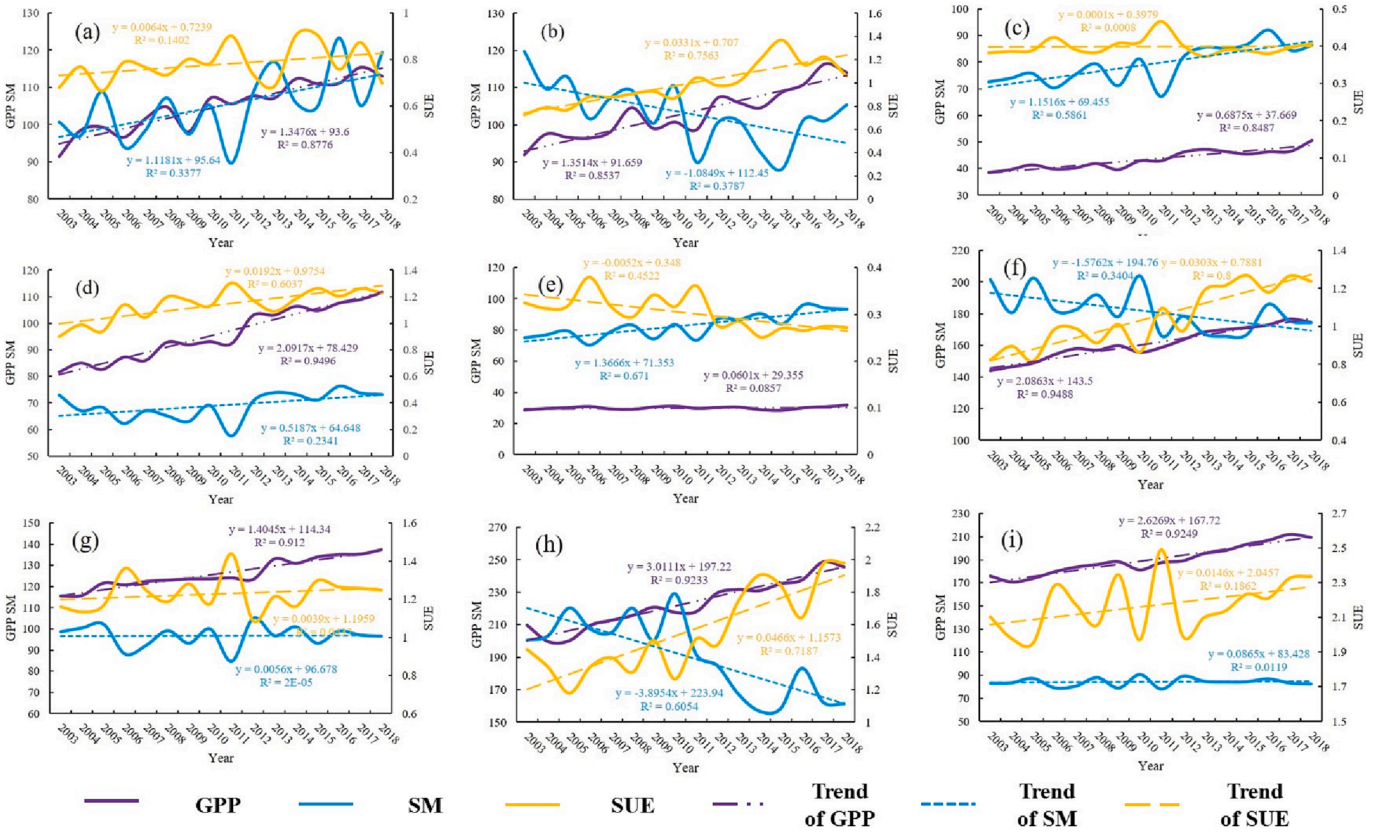

Fig. 2. Temporal variation characteristics of gross primary productivity (GPP), soil moisture content, and soil moisture use efficiency (SUE) in nine agricultural divisions.

moisture content change, the growth rate in the area north of Qinling and Huaihe River was much larger than that in the area south of Qinling and Huaihe River; this change state indicates that the climate in northern China is developing toward warming and humidification (Kang and Eltahir, 2018). The overall trend of GPP as a whole indicated that the growth of soil moisture content in northern China does not inhibit the growth of SUE. In the context of global warming, snow accumulation in the high mountains and glacier ablation in Region E greatly replenished the soil moisture content, but the regional GPP did not change significantly, resulting in a decreasing trend of SUE (Cui et al., 2022; Zheng and Zhang, 2022).

3.3. SUE of different soil types

The WUE of vegetation in different soil types is shown in Fig. 3. The highest SUE (1.83 g C/m^{-2} kg H_2O) was found for ferralisols, followed by luvisols (1.3 g C/m^{-2} kg H_2O), skeletoi primitive soils (0.98 g C/m^{-2} kg H_2O), semi-luvisols (0.94 g C/m^{-2} kg H_2O), anthrosols (0.92 g C/m^{-2} kg H_2O), dark semi-hydromorphic soils (0.76 g C/m^{-2} kg H_2O), hydromorphic soils (0.53 g C/m^{-2} kg H_2O), caliche soils (0.38 g C/m^{-2} kg H_2O), alpine soils (0.24 g C/m^{-2} kg H_2O), desert soils (0.2 g C/m^{-2} kg H_2O), and arid soils (0.17 g C/m^{-2} kg H_2O). Ferralisols are mainly concentrated in the humid tropical and subtropical regions at low latitudes, where rain and heat conditions are better, and vegetation grows vigorously, so vegetation SUE is at its highest. Arid soils and desert soils are mainly distributed in the inland areas of northwest China. Due to the harsh regional climatic conditions, annual precipitation does not exceed 200 mm. Meanwhile, arid soils have large pores and a poor ability to retain water. The vegetation in these areas consists of mainly arid and super-arid small semi-shrubs and shrubs, and this type of vegetation has a small leaf area and a low photosynthetic rate, so the SUE of arid soil vegetation is maintained at a low level. Overall, the SUE of vegetation under different soil types showed large variation due to the complex dynamics of water retention capacity, soil fertility, and regional climatic factors.

3.4. SUE of different vegetation types

The SUE of different types of vegetation is shown in Fig. 4. In general, the SUE of vegetation gradually increases with an increase in canopy vegetation, showing the characteristics of forest > scrub > cultivated vegetation > wetland > grassland. The SUE of different forest types differed significantly, in the order of tropical rainforest > broadleaf forest > mixed forest > coniferous forest, and showed a decrease with increasing latitude, with tropical rainforest being the highest (3.36 g C/m^{-2} kg H_2O), followed by subtropical monsoon evergreen broad-leaved forest (3.34 g C/m^{-2} kg H_2O), tropical monsoon forest (2.48 g C/m^{-2} kg H_2O), subtropical evergreen broad-leaved forest (2.18 g C/m^{-2} kg H_2O),

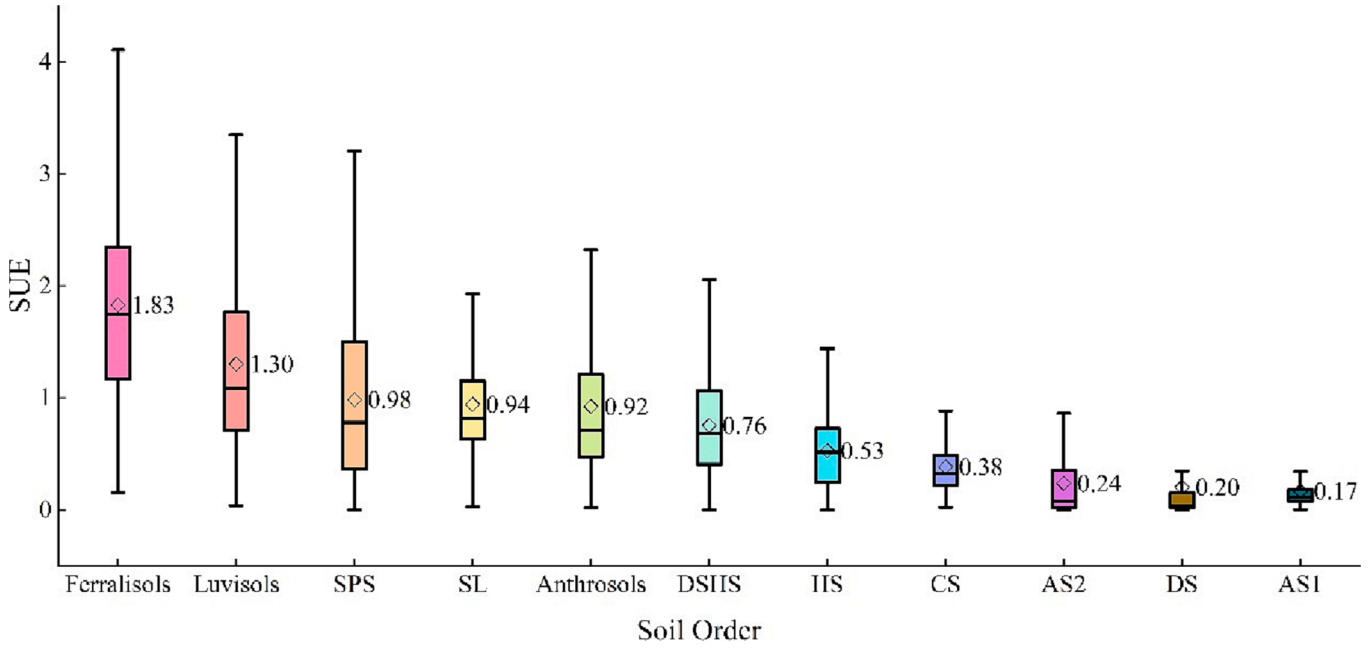

Fig. 3. SUE under different soil types.

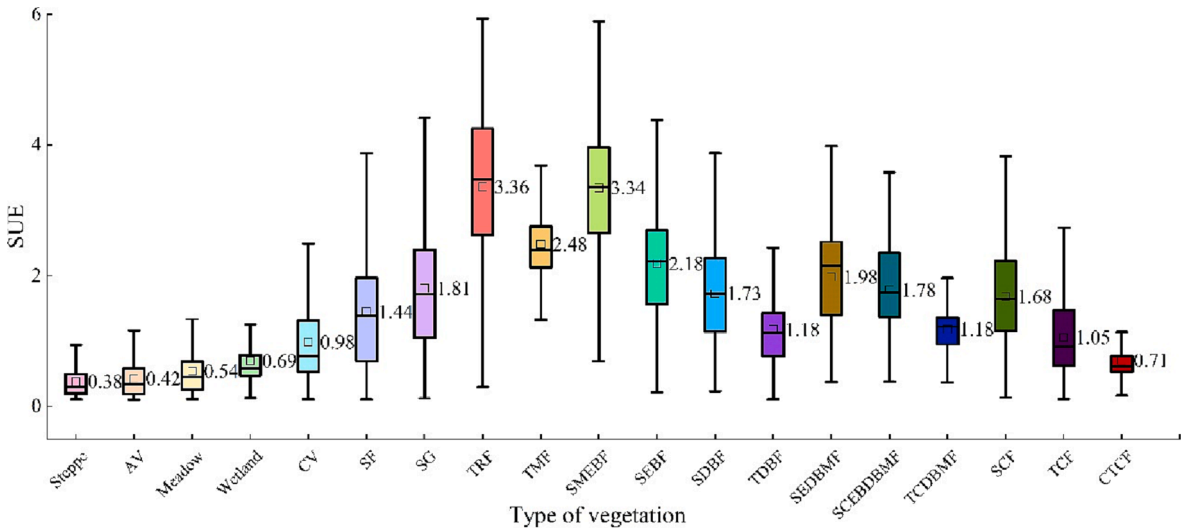

Fig. 4. SUE under different vegetation types.

subtropical evergreen deciduous broad-leaved mixed forest (1.98 g C/m^{-2} kg H_2O), subtropical coniferous evergreen broad-leaved deciduous broad-leaved mixed forest (1.78 g C/m^{-2} kg H_2O), subtropical deciduous broad-leaved forest (1.73 g C/m^{-2} kg H_2O), subtropical coniferous forest (1.68 g C/m^{-2} kg H_2O), temperate deciduous broad-leaved forest (1.18 g C/m^{-2} kg H_2O), temperate coniferous deciduous broad-leaved mixed forest (1.18 g C/m^{-2} kg H_2O), temperate coniferous forest (1.05 g C/m^{-2} kg H_2O), and cold temperate coniferous forest (0.71 g C/m^{-2} kg H_2O). Among shrub vegetation, the SUE was greater in shrub-grass (1.81 g C/m^{-2} kg H_2O) than in shrub forest (1.44 g C/m^{-2} kg H_2O). Cultivated vegetation receives high nutrients and water for growth under human control, guaranteeing that cultivated vegetation has relatively high SUE (0.98 g C/m^{-2} kg H_2O). Wetland vegetation (0.69 g C/m^{-2} kg H_2O), meadow (0.54 g C/m^{-2} kg H_2O), alpine vegetation (0.42 g C/m^{-2} kg H_2O), and steppe (0.38 g C/m^{-2} kg H_2O) showed low levels of SUE due to climatic and geographical factors.

3.5. SUE change attribution analysis

The relative contribution of GPP and soil moisture content, as direct factors affecting SUE, to the change in SUE is shown in Fig. 5. The relative contribution rate of GPP to SUE change was 82.13% of the total area with positive contribution, and 17.87% of the total area with negative contribution, where the average contribution of GPP to SUE change in the nine sub-districts was 42.32% (Region A), 41.06% (Region B), 40.97% (Region C), 64.76% (Region D), 11.96% (Region E), 40.45% (Region F), 32.01% (Region G), 49.88% (Region H), and 49.67% (Region I). The relative contribution of soil moisture content to SUE change was positive in approximately 29.1% of the total area and negative in approximately 70.9% of the total area, where the average contribution of soil moisture to SUE change in the nine subdivisions was −34.27% (Region A), −45.45% (Region B), 20.36% (Region C), −20.4% (Region D), −46.12% (Region E), 4.64% (Region F), −25.42% (Region G), 15.06% (Region H), and −16.64% (Region I). The relative contribution

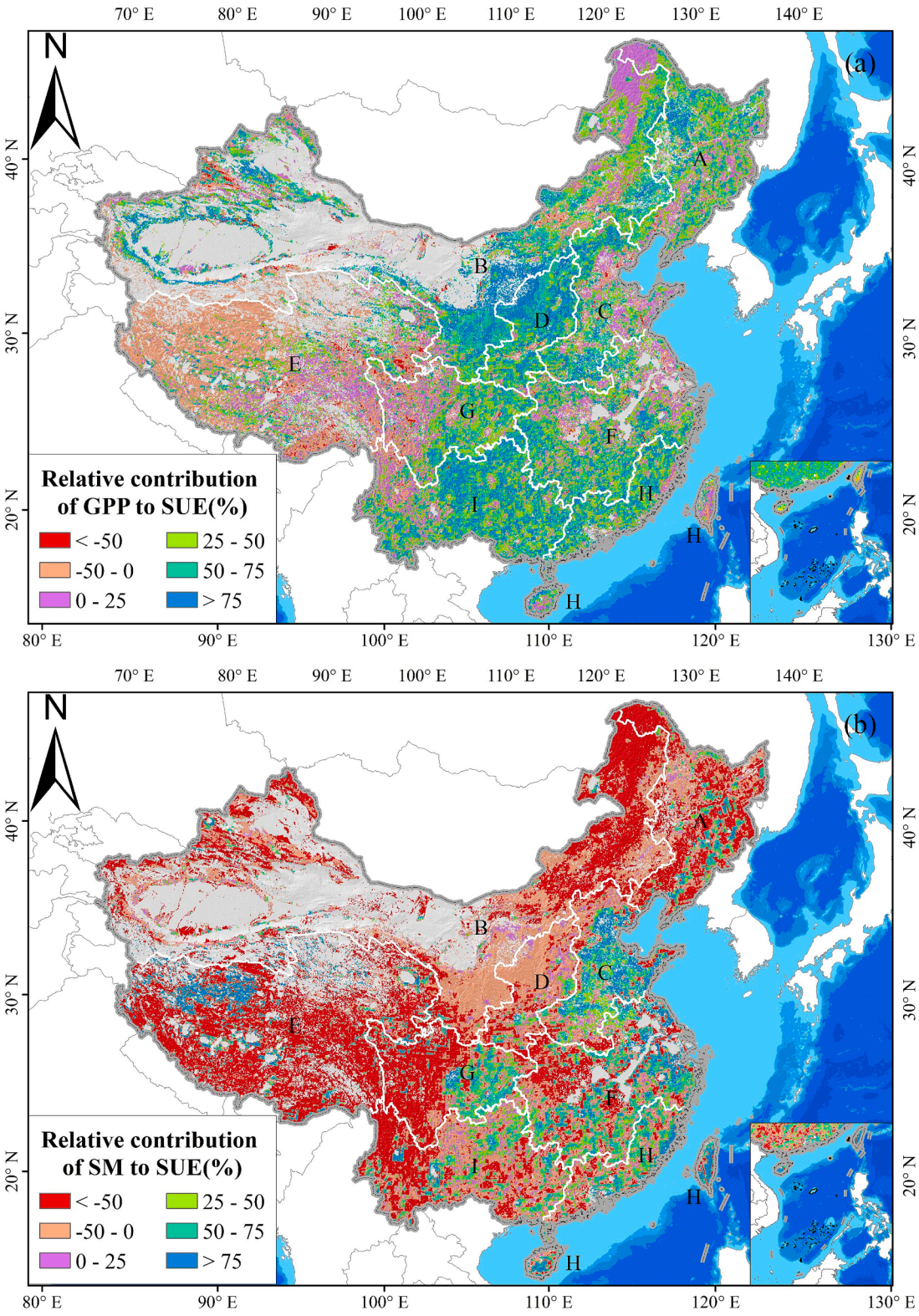

Fig. 5. Relative contribution of GPP (a) and soil moisture content (b) to the change in SUE.

of GPP to SUE change was positive in all nine sub-regions, meaning that SUE increased with GPP, especially in the northern part of Region A, the central part of Region B, the northern part of Region D, and the eastern part of Region I. The relative contribution of soil moisture content to SUE change was negative in Regions A, B, D, E, G, and I, meaning that SUE decreased with increasing soil moisture content. However, the relative contribution of soil moisture content to SUE change was positive in Regions C, Region H, southern Region F, southeastern Region A, central Region D, and eastern Region G. These regions are important food production bases in China (Sichuan Basin, Yellow and Huaihai Plains, Middle and Lower Yangtze River Plains, Guanzhong Plain, and Fen River Plain), and the addition of human activities is important to ensure crop yield. Therefore, both GPP and soil moisture content showed positive contributions to SUE in these regions. However,

changing the mechanism of the effect of soil moisture content on SUE under natural conditions in the above mentioned areas leads to many uncertainties in the contribution of soil moisture content to SUE.

For each subregion, the dominant factors affecting SUE changes accounted for the percentages shown in Fig. 6. Among them, the proportion of temperature change as the dominant factor was the highest in all sub-regions, especially in Region C, where temperature change as the dominant factor accounted for 45.5% of the whole region. In contrast, it was found that the percentage of regions with temperature change as the dominant factor was higher in southern China than in northern China, and the percentage of temperature change as the dominant factor had the characteristic of changing with decreasing latitude. In Regions A, B, and D, LAI was the second dominant factor affecting SUE variation; in Region C, the second dominant factor was net radiation, and the second dominant factor in the remaining regions was precipitation. In contrast, it was found that precipitation variation affected SUE to a much greater extent in the southern regions of China than in the northern regions. The reason for this phenomenon is that precipitation in the northern regions is lower than that in the southern regions, leading to the predominance of drought-tolerant vegetation in the northern regions and the relatively lower drought tolerance of vegetation in the southern regions. For the whole study area, temperature was the first dominant factor, precipitation was the second dominant factor, net radiation was the third dominant factor, LAI was the fourth dominant factor, and potential evapotranspiration was the fifth dominant factor affecting SUE variation. These results show that changes in hydrothermal conditions are the most important factors affecting the changes in SUE.

4. Discussion

4.1. Different analysis of PUE and SUE

The spatial distributions of SUE and PUE during different seasons are shown in Fig. 7. Both SUE and PUE showed not only obvious seasonal differences, but also maintained similar spatial distributions, gradually increasing from north to south, and the PUE and SUE were found to be much higher in southwest China (Region I) than in other regions. This conclusion is consistent with the findings of Liu et al. (2022) and Xue et al. (2022). The main reason for the higher vegetation WUE in southwest China compared to other regions is that southwest China is located in the subtropics and has a subtropical monsoon climate with good hydrothermal conditions, resulting in much higher species abundance than other regions. Polley et al. (2017) found that higher species abundance tends to represent more vigorous vegetation productivity and, due to the complementary law of ecological niches, higher species abundance implies faster water cycling, faster carbon and energy cycles, and higher PUE and SUE. The areas with relatively low PUE and SUE values were concentrated in Regions B and E. However, there are different reasons for the low SUE and PUE values in these two regions. Region E is the Qinghai-Tibet Plateau region, and the SUE and PUE showed overall distribution characteristics of high in the east and low in the west, high in the south and low in the north, which is greatly related to its elevation variation. With the elevation increase, precipitation decreases, temperature decreases, soil moisture content decreases, vegetation height decreases, LAI decreases, and many climatic factors and vegetation physiological factors that affect vegetation WUE decrease. The WUE of vegetation on the Qinghai-Tibet Plateau was therefore lower than that of other regions. Region B is an arid and semi-

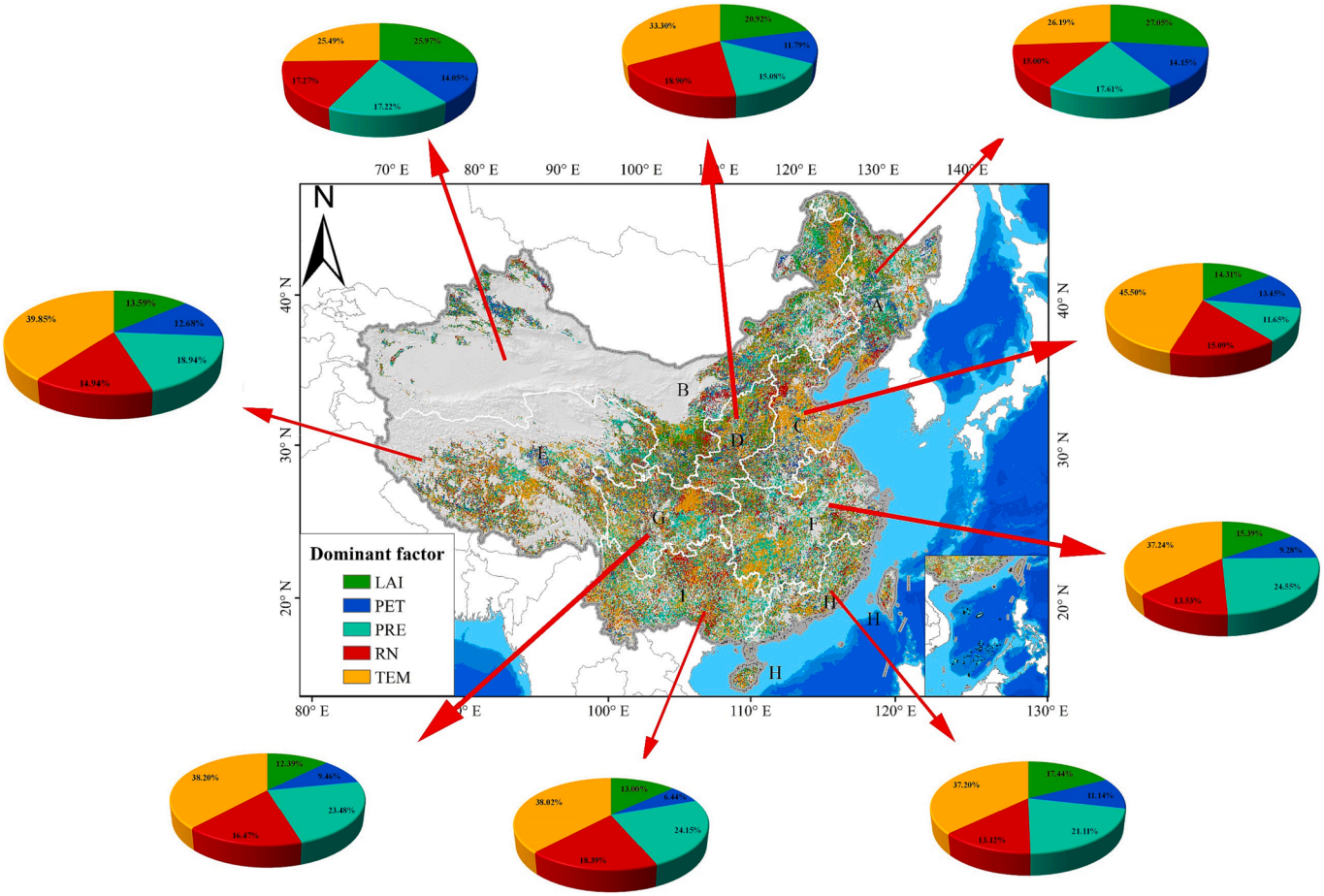

Fig. 6. Spatial distribution of leading climate factors affecting SUE changes.

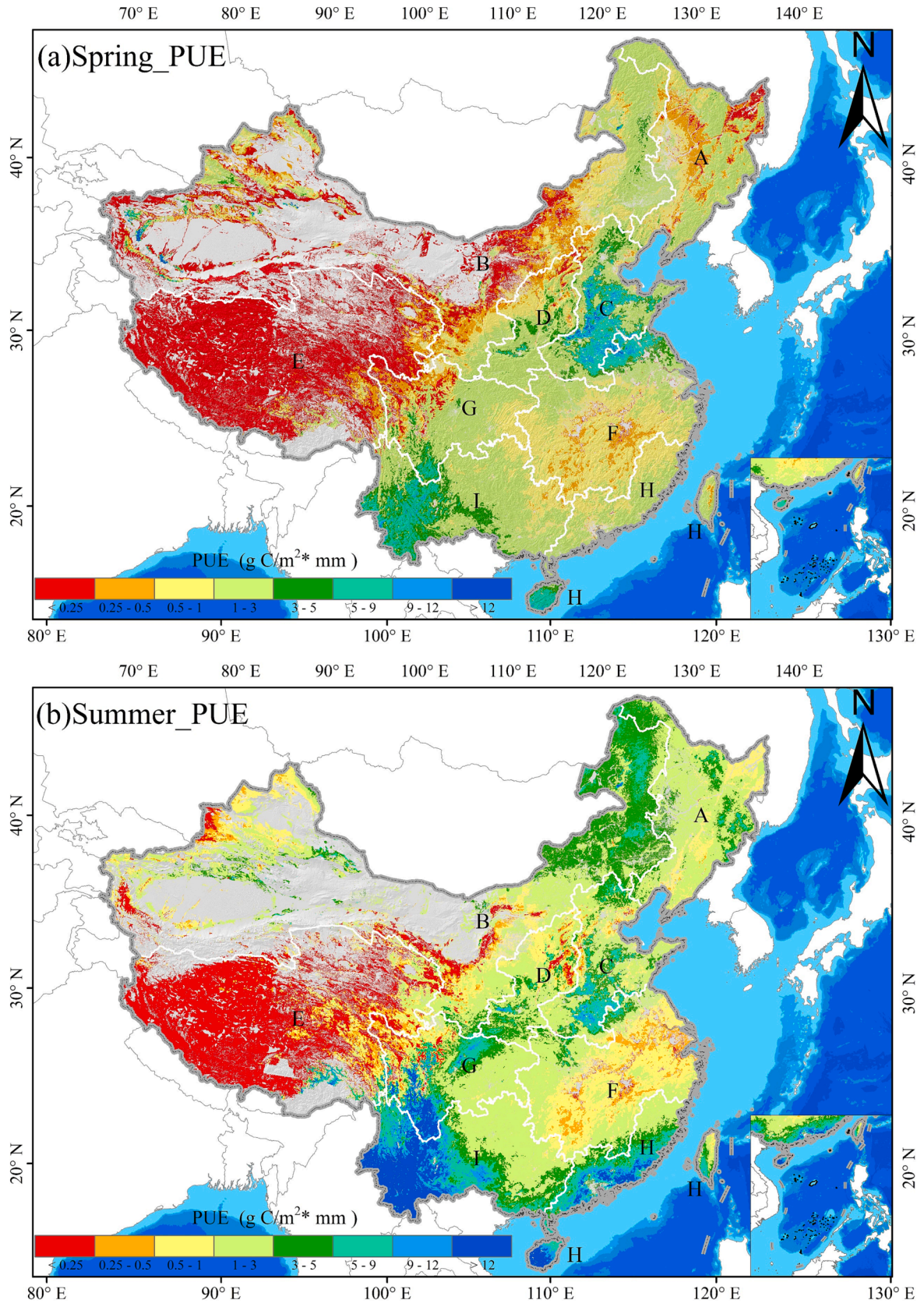

Fig. 7. Seasonal spatial distribution of SUE and PUE.

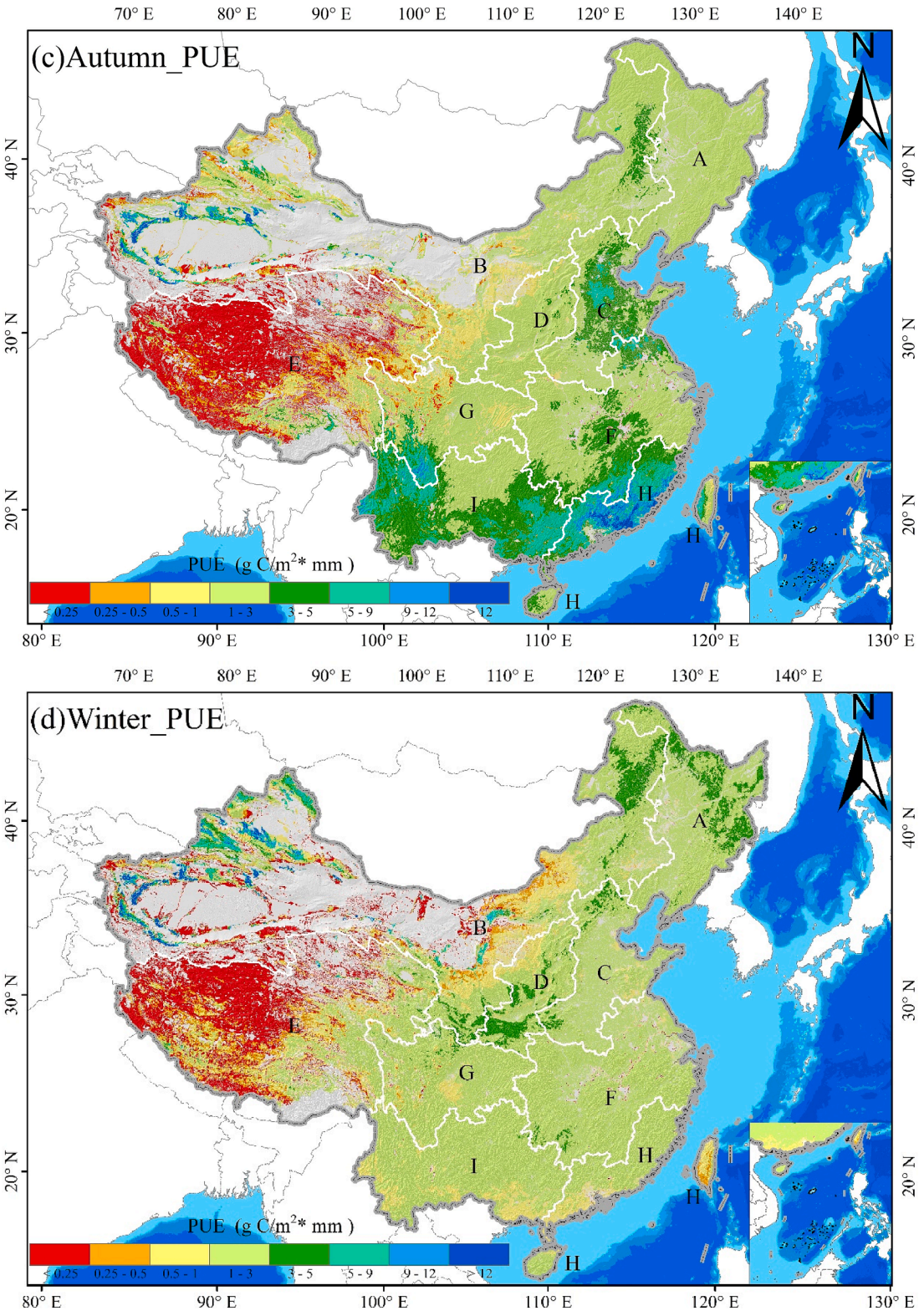

Fig. 7. (*continued*).

arid region in northern China, and the low WUE of vegetation in this region is not only related to the physiological characteristics of the local vegetation but is also influenced by the local climatic environment. Firstly, the vegetation in Region B has a large root to crown ratio, poor stomatal conductance, low photosynthetic efficiency, and weak carbon sequestration capacity (Dingkuhn et al., 2020). Secondly, the annual precipitation in the area is 300–500 mm, and the average annual evaporation is 260 mm, which greatly limits the physiological activity of vegetation and reduces the stability of the ecosystem due to water deficit (Hu et al., 2018).

On the seasonal scale, SUE and PUE showed unimodal patterns of variation, exhibiting the highest values in summer (SUE: 1.36, PUE: 2.43), followed by autumn (SUE: 0.63, PUE: 1.85), winter (SUE: 0.59, PUE: 1.4), and the lowest in spring (SUE: 0.34, PUE: 1.03). These

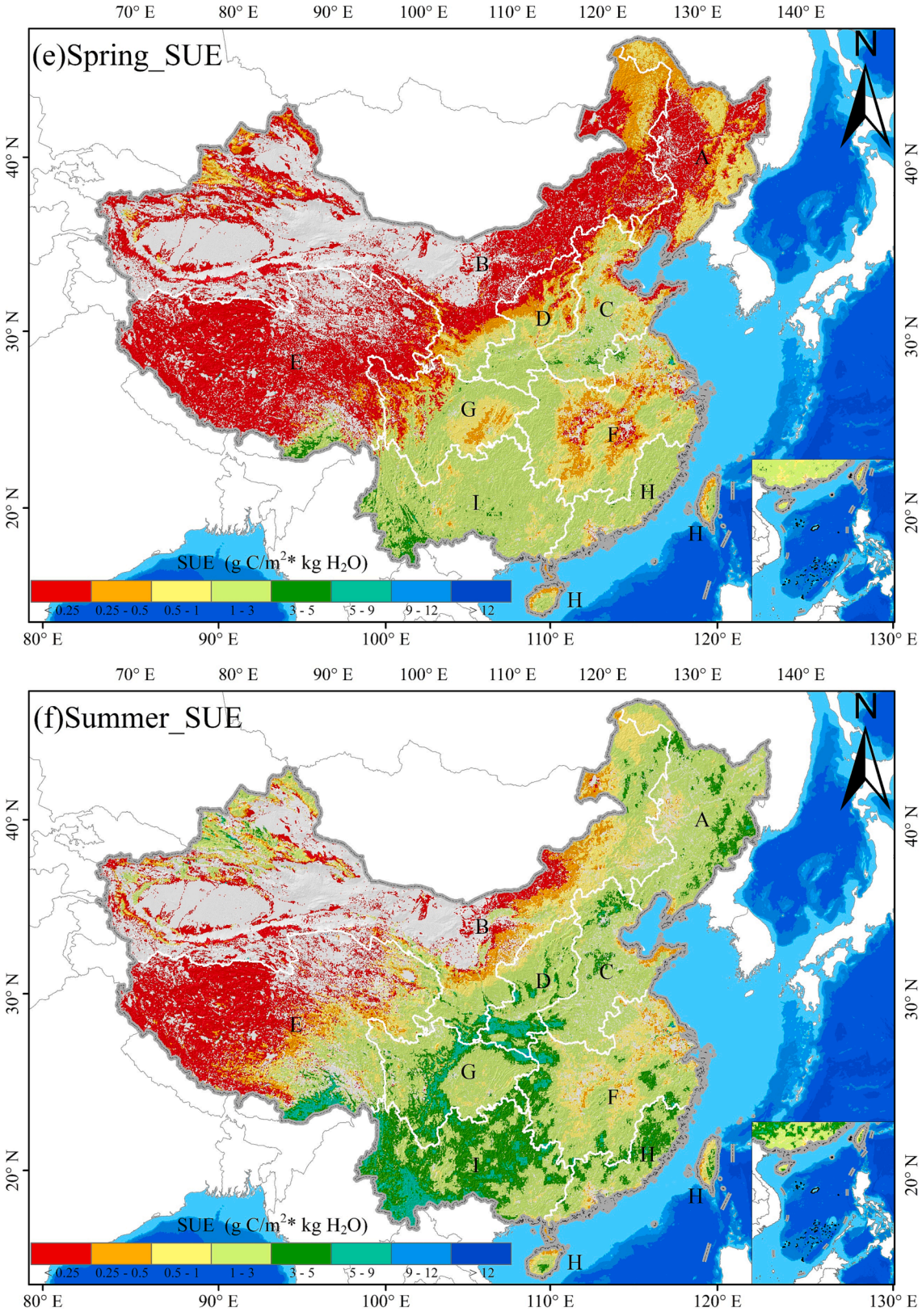

Fig. 7. (*continued*).

seasonal differences in vegetation WUE are consistent with the regional climatic characteristics of China. The comparison revealed that the spatial continuity of PUE was better than that of SUE, which was especially obvious in Region G (Sichuan Basin). The reason for this difference is that precipitation is spatially consistent in the region, while soil moisture is affected by other factors besides precipitation, including relative humidity, air temperature, wind speed, soil nutrients, soil texture, vegetation type, vegetation cover, water pressure, and topography, and the influence of multiple elements leads to poor spatial continuity of soil moisture content (Li et al., 2022). Relevant studies

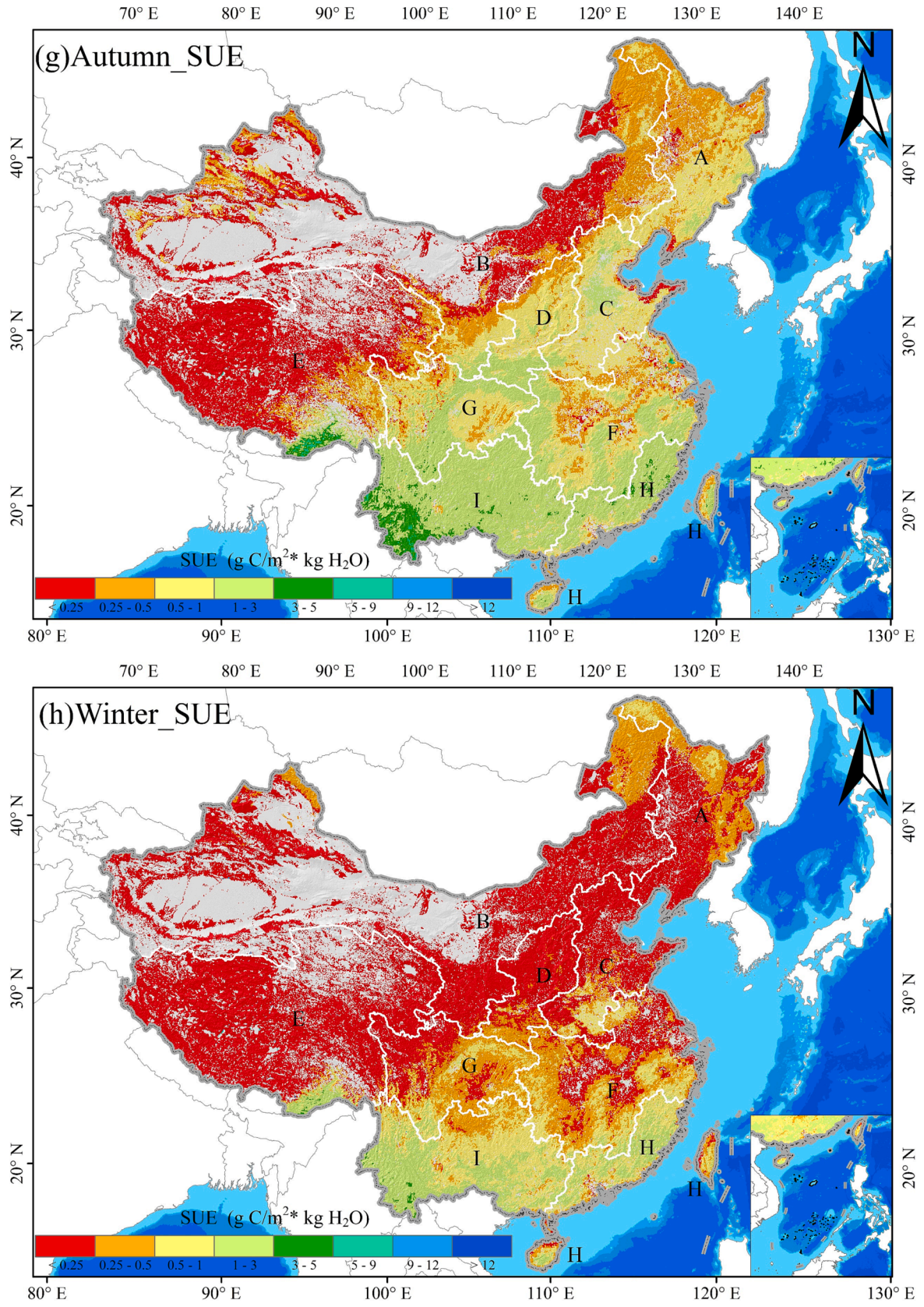

Fig. 7. (*continued*).

have shown that soil water in natural grassland is easily and effectively recharged. The efficiency of precipitation recharge is affected by factors such as leaf roughness, vegetation structure, and vegetation density. Similarly, the relatively low recharge efficiency in woodland due to canopy interception is also influenced by these factors. Therefore, effective recharge of soil water only occurs during periods of high

precipitation. Sandy land has strong and rapid infiltration, but low vegetation density and poor soil water retention capacity, resulting in a low soil water recharge efficiency (Zhou et al., 2020). In addition, the soil moisture transformed by precipitation is not completely used by vegetation, and the water that can be used by vegetation is limited to a certain depth of soil moisture. In summary, PUE has the characteristic of overestimating vegetation WUE compared with SUE, and its spatial distribution does not truly reflect vegetation WUE.

4.2. *Effect of climatic factors on GPP and soil moisture content*

Climate and environmental factors are important factors affecting the differences in spatial and temporal distribution of SUE, GPP, and soil moisture content as direct factors for inversion of SUE; therefore, it is necessary to analyze the effects of each climate factor on GPP and soil moisture content. Fig. 8 shows the relative contribution of each climatic element to GPP. The contribution of LAI to GPP was found to be high (>50%) in Regions A, B, D and F. The contribution of GPP to SUE was

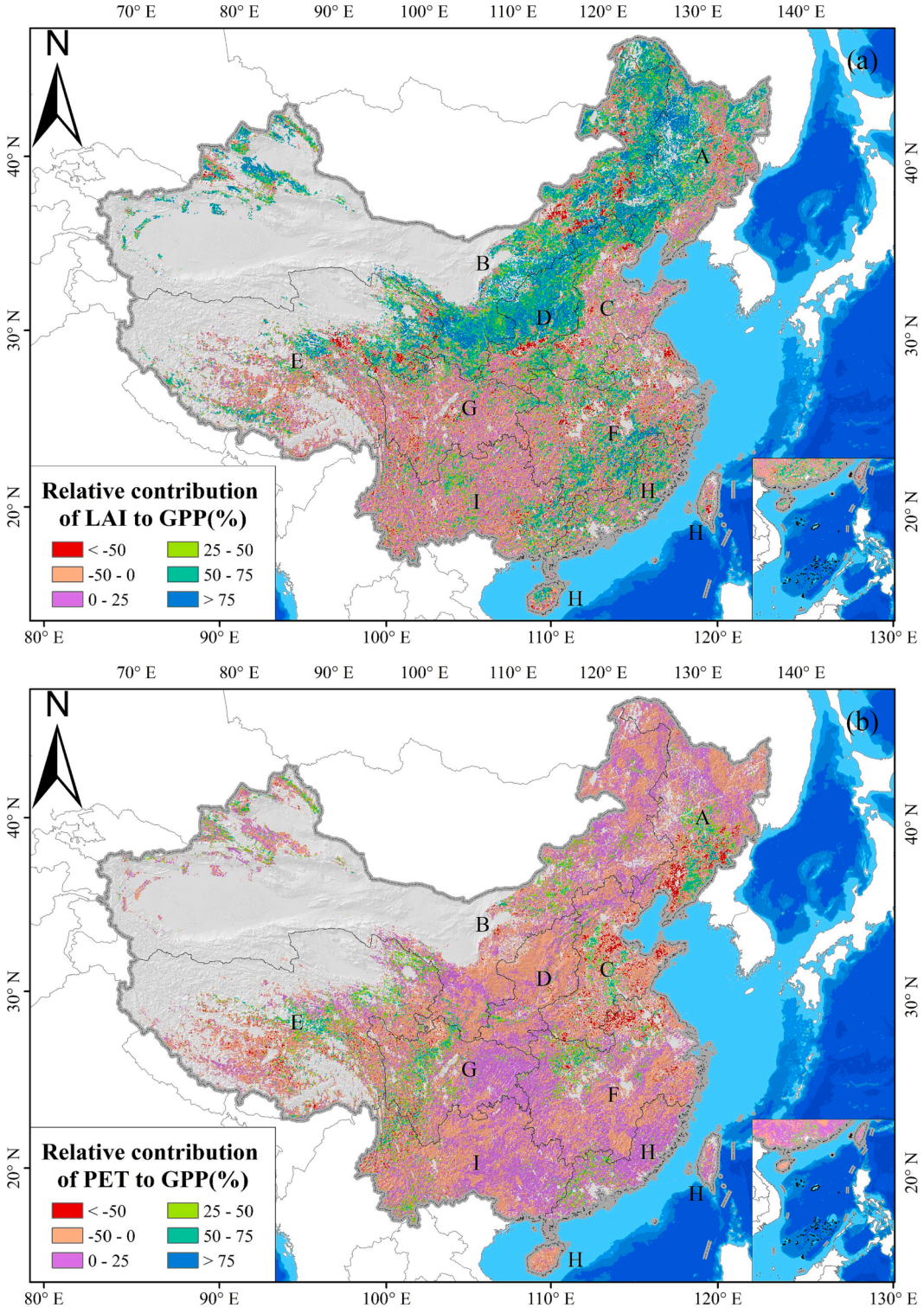

Fig. 8. Relative contribution of climate factors to GPP.

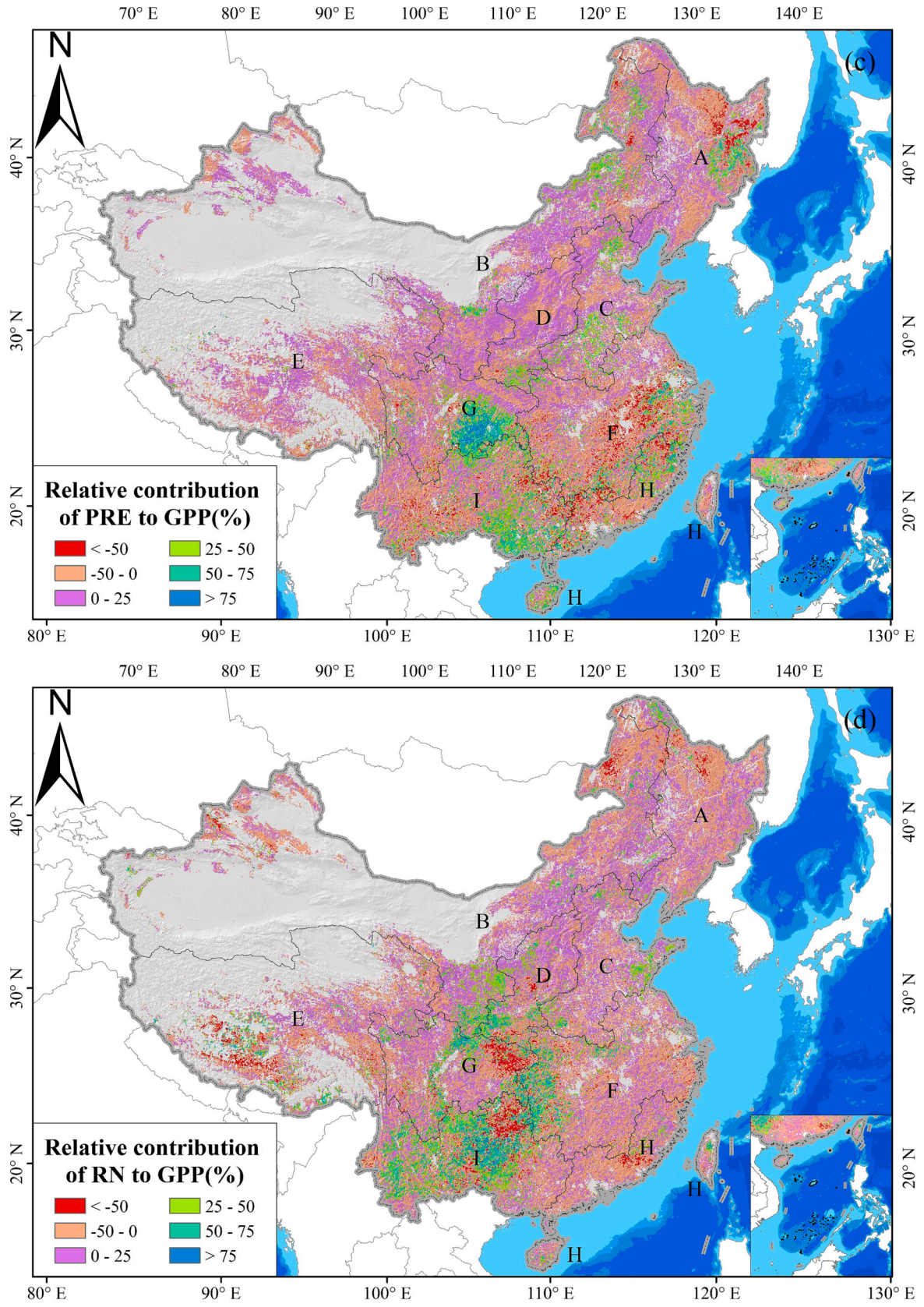

Fig. 8. (*continued*).

maintained at a high level in the above regions due to the continuous vegetation recovery in the above regions in recent years. The relative contribution of net radiation to GPP was higher in Region I than in other regions, remaining at 25%–75%. Zhang et al. (2022) found that RN was highest in southwest China (119.2 W/m^2), and lower in the Chuan-Qian Basin (east of Region G and north of Region I) and northwest China.

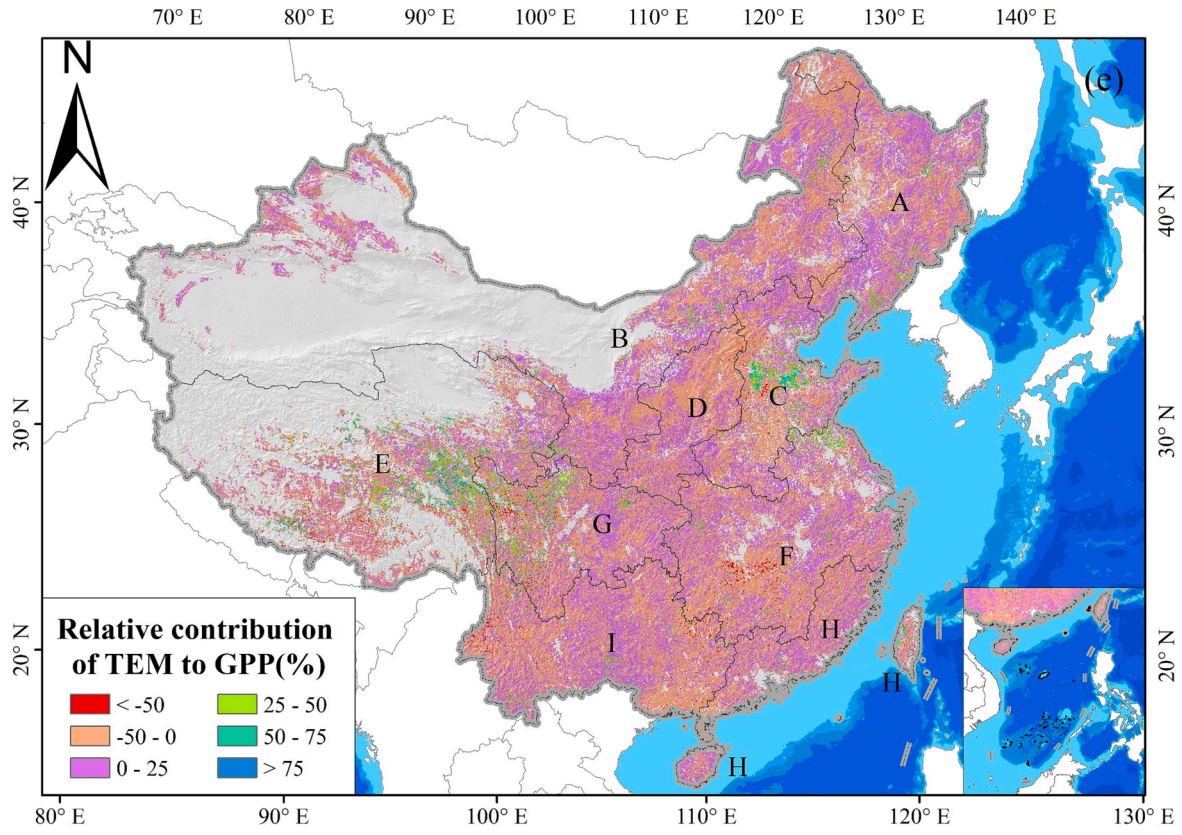

Fig. 8. (*continued*).

Meanwhile, the annual precipitation in southwest China is high, and the soil moisture content varies little; therefore, the net radiation becomes the dominant factor affecting GPP in Region I. The contribution of precipitation to GPP was higher in eastern Region G and eastern Region I compared to other regions. The relative contribution of potential evapotranspiration to GPP was higher in southern Region A, eastern Region E, and western Region G. The contribution of temperature to GPP remained largely in the range of 0%–25%. Overall, the average contributions of the five climate factors to GPP in the Chinese region were 23.96% for LAI, 1.08% for potential evapotranspiration, 3.01% for precipitation, 2.03% for RN, and 2.51% for temperature, with all factors contributing to the growth of GPP.

The relative contribution of climatic factors to soil moisture content is shown in Fig. 9, where the relative contribution of precipitation to soil moisture content was positive in most areas (Regions F, H, and I, eastern parts of Regions A and B, and southeastern part of Region G), and the contribution was greater than 50%. It is worth noting that the contribution of precipitation to soil moisture content was negative in Region C, which was caused by the continuous decline of the groundwater level in Region C (Feng et al., 2017). The North China Plain is an important grain producing area in China, where around 75% of the agricultural land is irrigated. Agricultural water use accounts for approximately 70% of the total regional water use, of which approximately 70% of agricultural water use comes from groundwater (Sun et al., 2010). Long-term groundwater extraction leads to a decrease in soil moisture holding capacity, and the limited precipitation recharges deep groundwater through infiltration. The other factors had positive contributions only locally, such as surface effective net radiation in the northwestern part of Region D, potential evapotranspiration in the central part of Region E, the northwestern part of Region I, and the southwestern part of Region C. Overall, the average contributions of the five factors to soil moisture content in the Chinese region were −1.07% for LAI, −1.28% for potential evapotranspiration, 15.37% for precipitation, −6.16% for RN, and −1.18% for temperature, with only precipitation contributing to soil moisture content and all other factors being inhibitory.

4.3. Impact of ecological engineering on SUE

The Chinese government has initiated a series of ecological projects since 1998, such as natural forest resource protection, the Grain for Green project, the construction of the Three-North Forest Protection System, the construction of the Yangtze River Forest Protection System, and the restoration of farmland to grassland (Bryan et al., 2018). As of 2019, the average vegetation cover in China is 53.3%, and the areas with increased vegetation cover are mainly located in the Northeast Plain (Fig. 10a), Loess Plateau (Fig. 10b), Sichuan Basin (Fig. 10c), and Yunnan-Guizhou Plateau (Fig. 10d). Shao et al. (2022) found that the average rate of change in vegetation net primary productivity (NPP) in China from 2000 to 2019 was 2.4 g C m^{-2} yr^{-1}, with a steady overall increase. The main areas of increase were concentrated in the northern arid and semi-arid regions, the Loess Plateau, the Yunnan-Guizhou Plateau, and the Sichuan Basin. Consistent with the trend of vegetation NPP, SUE in the Chinese region also maintained an increasing trend (9.17×10^{-3} g C/m^{-2} kg H_2O yr^{-1}). The relative contribution of ecological engineering to NPP growth was 14.6%, while in the Loess Plateau region it was more than 50% (Shao et al., 2022). Meanwhile, the relative contribution of GPP to SUE increase was 37.53% in this study and 64.76% in the Loess Plateau region. The implementation of ecological projects not only increases the vegetation cover and surface carbon sink capacity but also effectively improves the surface water source connotation capacity and enhances the soil and water conservation capacity (Feng et al., 2016). The contradiction between water supply and demand is a bottleneck that restricts the healthy development of the economy, society, and the ecological environment. Due to the uneven spatial and temporal distribution of precipitation in China, especially in the northwest inland areas where precipitation is low and

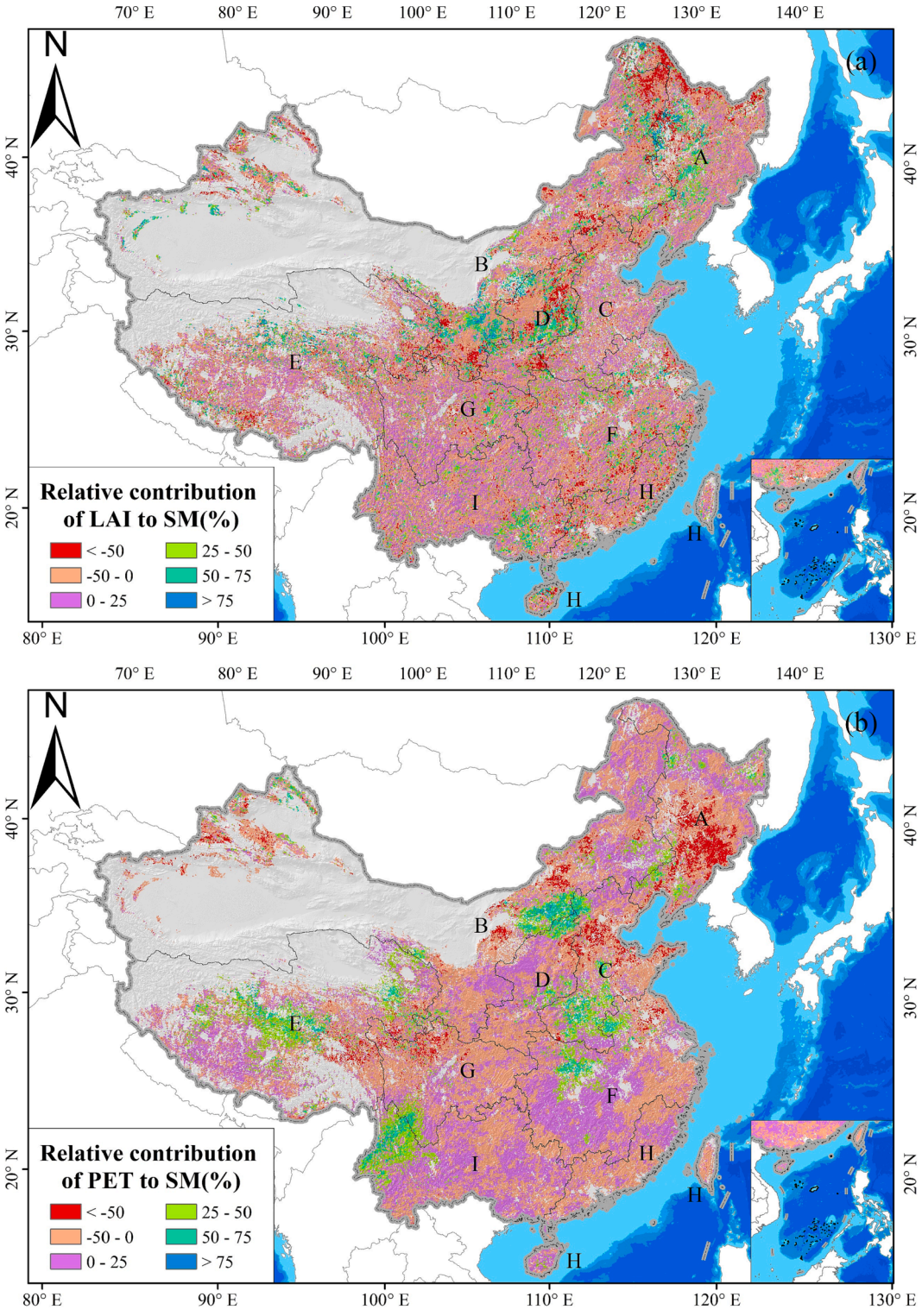

Fig. 9. Relative contribution of climate factors to soil moisture content.

land evapotranspiration is large, the spatial variation in soil moisture content is significant (Yang et al., 2021). The implementation of ecological projects may aggravate the loss of soil moisture; therefore, in water-scarce areas, we should optimize the allocation of water resources, promote efficient irrigation technology to develop intensive agricultural production modes, fully exploit the economic value of the ecological environment, and promote the sustainable development of the ecological environment rather than blindly implementing afforestation to increase the consumption of water resources (Huang et al., 2017; Xue et al., 2022). Thus, under the premise of guaranteeing the sustainable development of terrestrial ecosystems, we should insist on the self-restoration of ecosystems as the first solution to solve the numerous ecological problems that we face, especially in ecologically fragile areas.

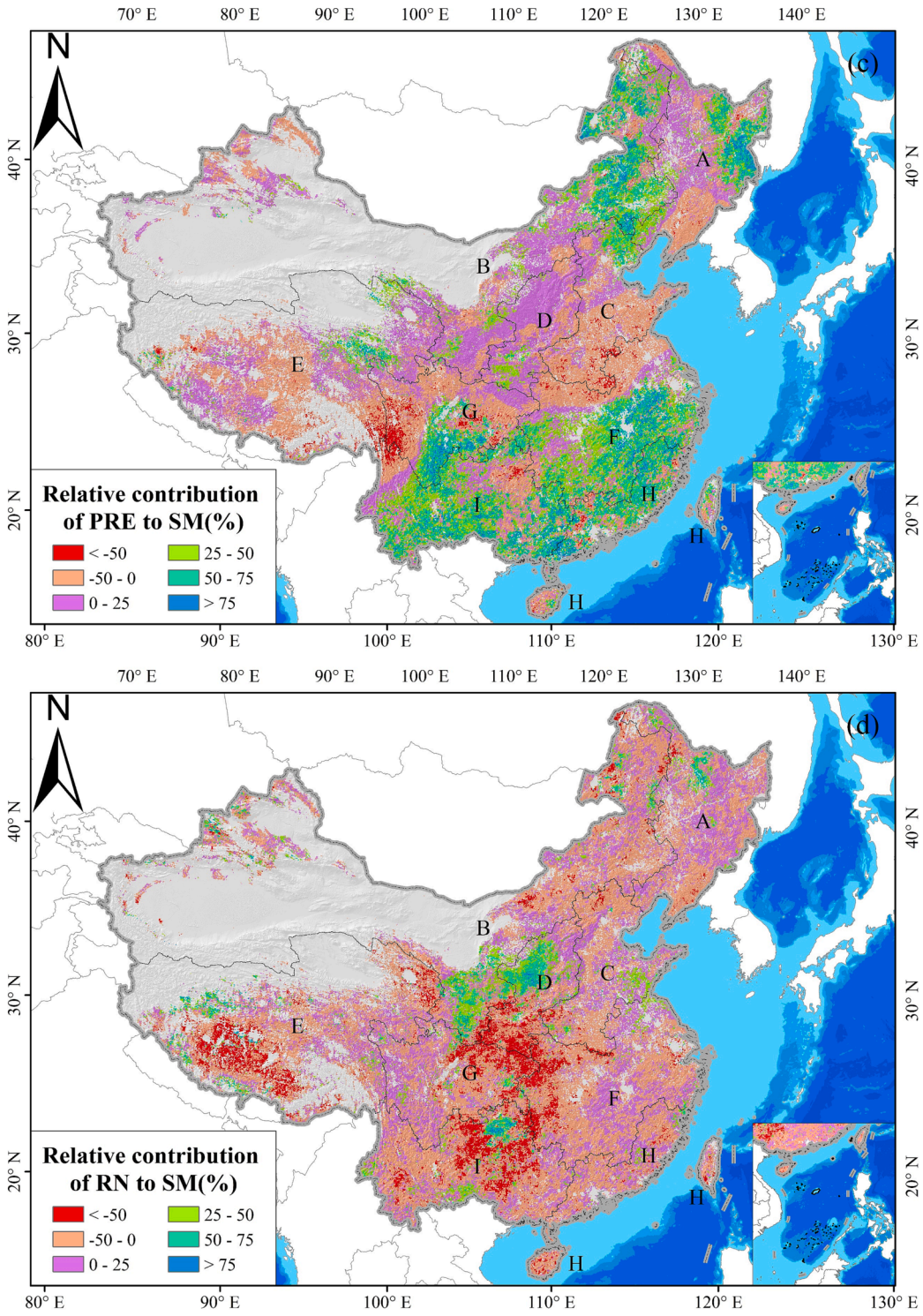

Fig. 9. (*continued*).

4.4. Uncertainty analysis of this study

In this study, vegetation WUE was inferred based on the soil moisture content, precipitation, and GPP data, and validated using flux site data, and the simulation results were consistent with the observations; however, some shortcomings remain. First, the soil moisture content data were not validated in this study; second, the limited number of observation sites and the small quantity of data had a great impact on the accuracy of the validation results. The remote sensing data used in this study had a spatial resolution of 0.05°, which could not quantify the characteristics of vegetation WUE in a small area, although it could reflect the characteristics of spatial distribution, except SUE and PUE. Besides that, all the climate data were sampled to 0.05° when the contribution analysis was conducted, and the sampling results may have led to a shift in the spatial location of the SUE and climate data, which brings many uncertainties to the experimental results. Therefore, in future studies, higher resolution remote sensing data and more flux site data should be considered, and experiments on soil moisture content measurements in the field should be included.

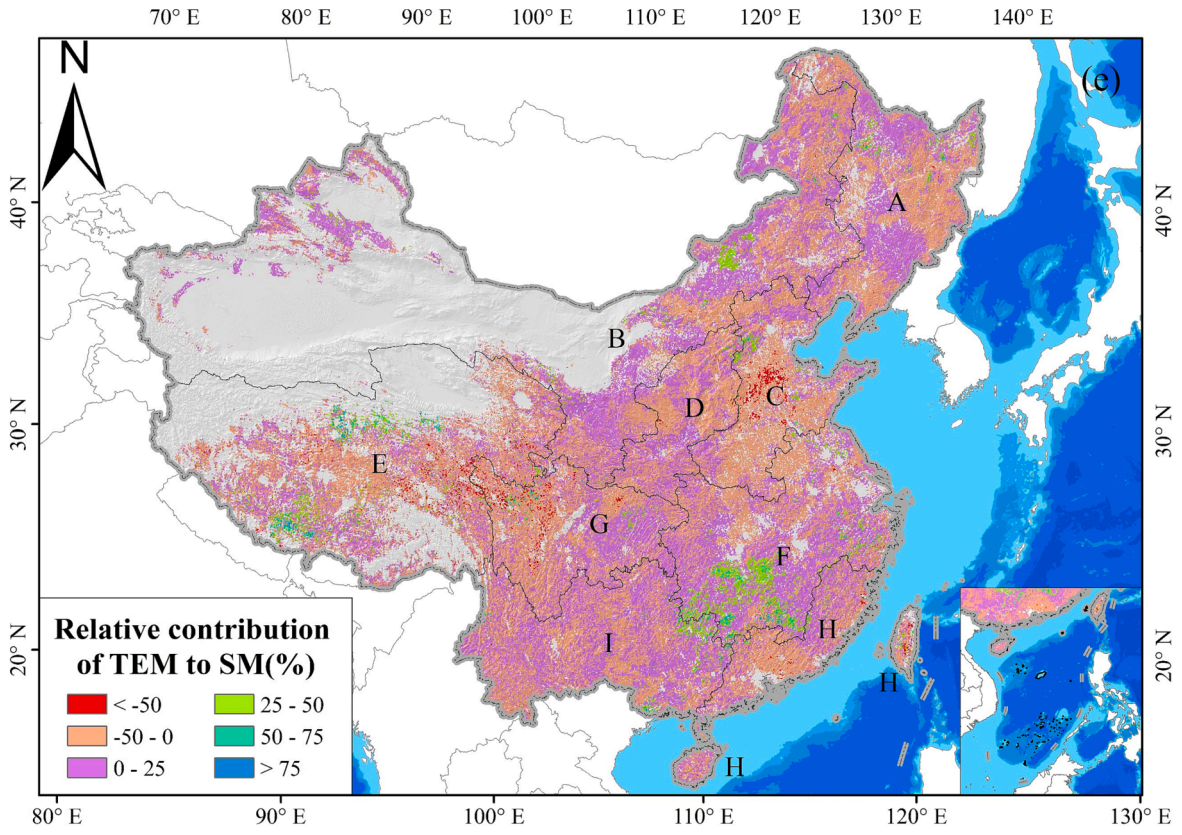

Fig. 9. (*continued*).

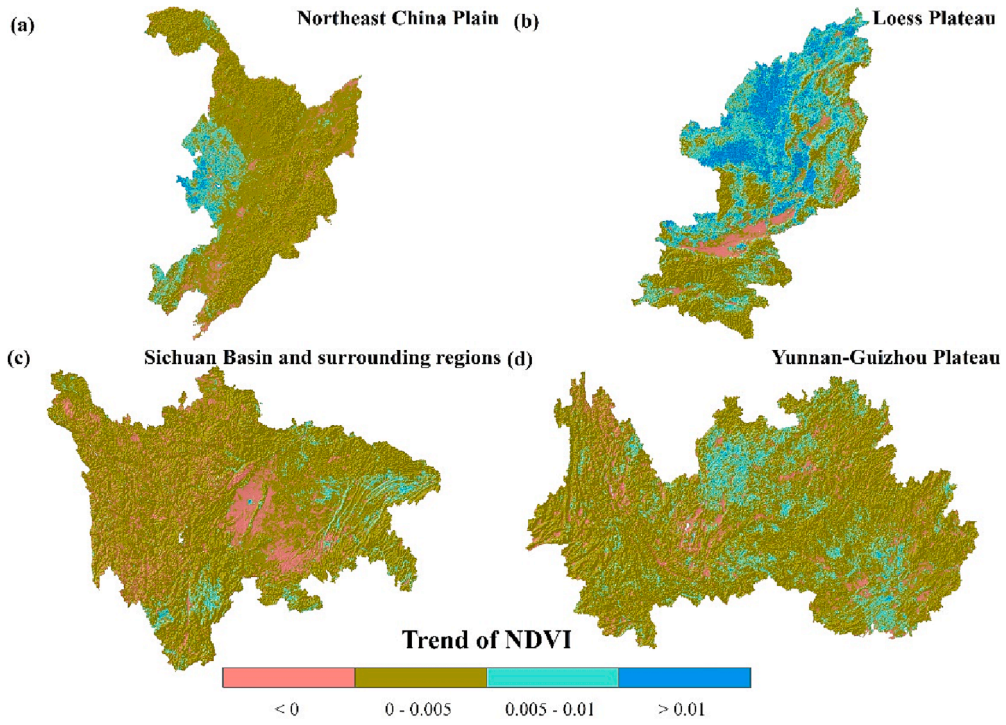

Fig. 10. The spatial distribution characteristics of NDVI trends in different regions.

5. Conclusions

In this study, PUE and SUE were calculated for the Chinese region using GOSIF GPP, soil moisture content, and precipitation data. The SUE was verified using flux site data, and the relative contributions of GPP and soil moisture content to SUE, as well as the differences in the response of SUE to climate factors, were analyzed using the first-difference method. The results revealed the following:

(1) Among the nine stations, the correlation coefficients between SUERS and SUEST were greater than 0.75 among all stations, except the NMG station, and all passed the 99% significance test.
(2) Among the nine major agricultural sub-regions in China, only the SUE in the Qinghai-Tibet Plateau showed a decreasing trend, while all other regions maintained a growing trend. The fastest growth rate was in southern China.
(3) The WUE of vegetation under different types of soil was highest for ferralisols (1.83 g C/m^{-2} kg H_2O) and lowest for arid soils (0.17 g C/m^{-2} kg H_2O).
(4) The SUE of vegetation gradually increases as the vegetation canopy rises, showing the characteristics of forest > scrub > cultivated vegetation > wetland > grassland.
(5) The relative contribution of GPP to the change in SUE was 37.53%, while the relative contribution of soil moisture content to the change in SUE was −26.71%. Among the five climatic factors, temperature was the first dominant factor affecting the change in SUE, followed by precipitation, net surface radiation, LAI, and potential evapotranspiration.

CRediT authorship contribution statement

Hao Ding: Methodology, Formal analysis, Data curation, Writing – original draft. **Zhe Yuan:** Conceptualization, Writing – original draft, Funding acquisition, Project administration. **Xiaoliang Shi:** Methodology, Conceptualization, Funding acquisition, Supervision. **Jun Yin:** Investigation, Writing – review & editing, Funding acquisition. **Fei Chen:** Writing – review & editing. **Mengqi Shi:** Visualization, Resources. **Fulong Zhang:** Writing – review & editing, Resources.

Declaration of Competing Interest

The authors declare that they have no known competing financial interests or personal relationships that could have appeared to influence the work reported in this paper.

Data availability

The authors do not have permission to share data.

Acknowledgments

This research was funded by the National Key Research and Development Project (2022YF3201704), the National Natural Science Foundation of China (41890821, 52079008), and National Public Research Institutes for Basic R&D Operating Expenses Special Project (CKSF2023311/HL).

References

An, X., 2022. Responses of Water Use Efficiency to climate change in evapotranspiration and transpiration ecosystems. Ecol. Ind. 141, 109157 https://doi.org/10.1016/j.ecolind.2022.109157.
Bryan, B.A., Gao, L., Ye, Y., Sun, X., Connor, J.D., Crossman, N.D., Stafford-Smith, M., Wu, J., He, C., Yu, D., Liu, Z., Li, A., Huang, Q., Ren, H., Deng, X., Zheng, H., Niu, J., Han, G., Hou, X., 2018. China's response to a national land-system sustainability emergency. Nature 559 (7713), 193–204.
Chen, Y., Feng, X., Tian, H., Wu, X., Gao, Z., Feng, Y.u., Piao, S., Lv, N., Pan, N., Fu, B., 2021. Accelerated increase in vegetation carbon sequestration in China after 2010: A turning point resulting from climate and human interaction. Glob. Chang. Biol. 27 (22), 5848–5864.
Cui, Q., He, Y.and Li, Z., (2022). Spatial-temporal variation of vegetation water use efficiency and its relationship with climate factors over the Qinghai-Tibet Plateauu, China. Chinese J. Appl. Ecol., 33(6): 1525-1532.(in Chinese). DOI: https://10.13287/j.1001-9332.202206.024.
de Oliveira, G., Brunsell, N.A., Sutherlin, C.E., Crews, T.E., DeHaan, L.R., 2018. Energy, water and carbon exchange over a perennial Kernza wheatgrass crop. Agr. Forest Meteorol. 249, 120–137.
Dingkuhn, M., Luquet, D., Fabre, D., Muller, B., Yin, X., Paul, M.J., 2020. The case for improving crop carbon sink strength or plasticity for a CO2-rich future. Curr. Opin. Plant Biol. 56, 259–272.
Fang, J., Yu, G., Liu, L., Hu, S., Chapin, F.S., 2018. Climate change, human impacts, and carbon sequestration in China. Proc. Natl. Acad. Sci. USA 115 (16), 4015–4020.
Feng, W., Wang, C., Mu, D. et al., (2017). Groundwater storage variations in the North China Plain from GRACE with spatial constraints. Chinese J. Geophys., 60(5): 1630-1642.(in Chinese). DOI: https://10.6038/cjg20170502.
Feng, X., Fu, B., Piao, S., Wang, S., Ciais, P., Zeng, Z., Lü, Y., Zeng, Y., Li, Y., Jiang, X., Wu, B., 2016. Revegetation in China's Loess Plateau is approaching sustainable water resource limits. Nat. Clim. Chang. 6 (11), 1019–1022.
Fenger-Nielsen, R., Hollesen, J., Matthiesen, H., Andersen, E.A.S., Westergaard-Nielsen, A., Harmsen, H., Michelsen, A., Elberling, B.o., 2019. Footprints from the past: The influence of past human activities on vegetation and soil across five archaeological sites in Greenland. Sci. Total Environ. 654, 895–905.
Fu, C., Bian, Z., Xi, J., et al., 2018. Spatial distribution characteristics of soil moisture in different types of sand dune in the Mu Us Sandy Land, adjacent to north of Chinese Loess Plateau. Environ. Earth Sci. 77 (4), 1–12. https://doi.org/10.1007/s12665-018-7307-8.
Gao, Y., Zhu, X., Yu, G., He, N., Wang, Q., Tian, J., 2014. Water use efficiency threshold for terrestrial ecosystem carbon sequestration in China under afforestation. Agr. Forest Meteorol. 195-196, 32–37.
Gu, C., Tang, Q., Ma, G.Z.J. et al., (2021). Discrepant responses between evapotranspiration-and transpiration-based ecosystem water use efficiency to interannual precipitation fluctuations. Agr Forest. Meteorol., 303: 108385. 10.1016/j.agrformet.2021.108385.
Guerrieri, R., Belmecheri, S., Ollinger, S.V., Asbjornsen, H., Jennings, K., Xiao, J., Stocker, B.D., Martin, M., Hollinger, D.Y., Bracho-Garrillo, R., Clark, K., Dore, S., Kolb, T., Munger, J.W., Novick, K., Richardson, A.D., 2019. Disentangling the role of photosynthesis and stomatal conductance on rising forest water-use efficiency. Proc. Natl. Acad. Sci. USA 116 (34), 16909–16914.
Hatfield, J.L., Dold, C., 2019. Water-use efficiency: advances and challenges in a changing climate. Front. Plant Sci. 10, 103. https://doi.org/10.3389/fpls.2019.00103.
Heimann, M., Reichstein, M., 2008. Terrestrial ecosystem carbon dynamics and climate feedbacks. Nature 452 (7176), 289–292. https://doi.org/10.1038/nature06591.
Hou, Q., Pei, T., Yu, X. et al., (2022). The seasonal response of vegetation water use efficiency to temperature and precipitation in the Loess Plateau, China. Glob. Ecol. Conserv., 33: e01984. 10.1016/j.gecco.2021.e01984.
Hu, Z., Zhou, J., Zhang, L. et al., (2018). Climate dry-wet change and drought evolution characteristics of different dry-wet areas in northern China. Acta Ecol. Sinica, 38(6): 1908-1919.(in Chinese). DOI: https://10.5846/stxb201702260315.
Huang, J., Yu, H., Dai, A., et al., 2017. rylands face potential threat under 2 C global warming target. Nat. Clim. Chang. 7 (6), 417–422. https://doi.org/10.1038/nclimate3275.
Ji, Z., Pei, T., Chen, Y., Wu, H., Hou, Q., Shi, F., Xie, B., Zhang, J., 2022. The driving factors of grassland water use efficiency along degradation gradients on the Qinghai-Tibet Plateau, China. Global Ecol. Conserv. 35, e02090.
Kang, S., Eltahir, E.A.B., 2018. North China Plain threatened by deadly heatwaves due to climate change and irrigation. Nat. Commun. 9 (1), 1–9. https://doi.org/10.1038/s41467-018-05252-y.
Li, Z., Chen, Y., Zhang, Q. et al., (2020). Spatial patterns of vegetation carbon sinks and sources under water constraint in Central Asia. J. Hydrol., 590: 125355. 10.1016/j.jhydrol.2020.125355.
Li, J., Guo, X., Chuai, X. et al., (2021). Reexamine China's terrestrial ecosystem carbon balance under land use-type and climate change. Land Use Policy, 102: 105275. 10.1016/j.landusepol.2020.105275.
Li, X., Chu, J., Zhang, T. et al., (2022). Spatio-temporal evolution trend of groundwater drought and its dynamic response to meteorological drought in Northwest China. Water Resour. Protect., 38(1): 34-42.(in Chinese). DOI:https://10.3880/j.issn.1004-6933.2022.01.005.
Li, S., He, P., Liu, B., et al., 2016. Modeling of maize gross primary production using MODIS imagery and flux tower data. Int. J. Agr. Biol. Eng. 9 (9), 110–118. https://doi.org/10.3965/j.ijabe.20160902.2245.
Li, X., Xiao, J., 2019. Mapping photosynthesis solely from solar-induced chlorophyll fluorescence: A global, fine-resolution dataset of gross primary production derived from OCO-2. Remote Sens 11 (21), 2563. https://doi.org/10.3390/rs11212563.
Liu, Y., Chen, Q., Ge, Q., Dai, J., Qin, Y.a., Dai, L., Zou, X., Chen, J., 2018. Modelling the impacts of climate change and crop management on phenological trends of spring and winter wheat in China. Agr. Forest. Meteorol. 248, 518–526.
Liu, X., Lai, Q., Yin, S. et al., (2022). Exploring grassland ecosystem water use efficiency using indicators of precipitation and soil moisture across the Mongolian Plateau. Ecol. Indic., 142: 109207. 10.1016/j.ecolind.2022.109207.
LucLambs, (2004). Interactions between groundwater and surface water at river banks and the confluence of rivers. J. Hydrol., 288(3-4): 312-326. 10.1016/j.jhydrol.2003.10.013.
Mei, X., Ma, L., 2022. Effect of afforestation on soil water dynamics and water uptake under different rainfall types on the Loess hillslope. Catena 213, 106216. https://doi.org/10.1016/j.catena.2022.106216.
Meng, X., Mao, K., Meng, F., Shi, J., Zeng, J., Shen, X., Cui, Y., Jiang, L., Guo, Z., 2021. A fine-resolution soil moisture dataset for China in 2002–2018. Earth Syst. Sci. Data 13 (7), 3239–3261.
Nandy, S., Saranya, M., Srinet, R., 2022. Spatio-temporal variability of water use efficiency and its drivers in major forest formations in India. Remote Sens. Environ. 269, 112791 https://doi.org/10.1016/j.rse.2021.112791.
Polley, H.W., Adler, P.R., Scherer-Lorenzen, M., et al., 2017. Benefits of increasing plant diversity in sustainable agroecosystems. J. Ecol. 105 (4), 871–879. https://doi.org/10.1111/1365-2745.12789.

Qin, P., Xu, H., Liu, M. et al., (2020). Assessing concurrent effects of climate change on hydropower supply, electricity demand, and greenhouse gas emissions in the Upper Yangtze River Basin of China. Appl. Energ, 279: 115694. 10.1016/j.apenergy.2020.115694.

Shao, Q., Liu, S., Ning, J. et al., (2022). Assessment of ecological benefits of key national ecological projects in China in 2000-2019 using remote sensing. Acta Geogr. Sinica, 77(9): 2133-2153.(in Chinese). DOI:https://10.11821/dlxb202209001.

Song, Q.-H., Fei, X.-H., Zhang, Y.-P., Sha, L.-Q., Liu, Y.-T., Zhou, W.-J., Wu, C.-S., Lu, Z.-Y., Luo, K., Gao, J.-B., Liu, Y.-H., 2017. Water use efficiency in a primary subtropical evergreen forest in Southwest China. Sci. Rep.-UK 7 (1). https://doi.org/10.1038/srep43031.

Sun, X., Wang, G., Huang, M. et al., (2020). The asynchronous response of carbon gain and water loss generate spatio-temporal pattern of WUE along elevation gradient in southwest China. J. Hydrol., 581: 124389. 10.1016/j.jhydrol.2019.124389.

Sun, H., Shen, Y., Yu, Q., Flerchinger, G.N., Zhang, Y., Liu, C., Zhang, X., 2010. Effect of precipitation change on water balance and WUE of the winter wheat–summer maize rotation in the North China Plain. Agr. Water Manage. 97 (8), 1139–1145.

Tougeron, K., Brodeur, J., Le Lann, C., Baaren, J., 2020. How climate change affects the seasonal ecology of insect parasitoids. Ecol. Entomol. 45 (2), 167–181.

Van der Sleen, P., Groenendijk, P., Vlam, M., et al., 2015. No growth stimulation of tropical trees by 150 years of CO2 fertilization but water-use efficiency increased. Nat. Geosci. 8 (1), 24–28. https://doi.org/10.1038/NGEO2313.

Wang, L., Zhu, Q., Zhang, J. et al., (2023). Characteristics of water use efficiency during the changing process of vegetation in the Yellow River Basin. Acta Ecol. Sinica, 43 (8): 1-13.(in Chinese). DOI:https://10.5846/stxb202201040020.

Xia, J., Wang, J., Niu, S., 2020. Research challenges and opportunities for using big data in global change biology. Glob. Chang. Biol. 26 (11), 6040–6061. https://doi.org/10.1111/gcb.15317.

Xiao, J., Chevallier, F., Gomez, C. et al., (2019). Remote sensing of the terrestrial carbon cycle: A review of advances over 50 years. Remote Sens. Environ., 233: 111383. 10.1016/j.rse.2019.111383.

Xue, Y., Liang, H., Zhang, B. et al., (2022). Vegetation restoration dominated the variation of water use efficiency in China. J. Hydrol., 612: 128257. 10.1016/j.jhydrol.2022.128257.

Yang, J., Xie, B., Zhang, D., et al., 2021. Climate and land use change impacts on water yield ecosystem service in the Yellow River Basin, China. Environ. Earth Sci. 80 (3), 1–12. https://doi.org/10.1007/s12665-020-09277-9.

Yu, G., Chen, Z., Piao, S., Peng, C., Ciais, P., Wang, Q., Li, X., Zhu, X., 2014. High carbon dioxide uptake by subtropical forest ecosystems in the East Asian monsoon region. Proc. Natl. Acad. Sci. USA 111 (13), 4910–4915.

Zhang, X., Shen, B., Huang, L. et al., (2022). Estimation of surface net radiation and its spatio-temporal variation characteristics over Mainland China. J. Basic Sci. Eng., 30 (4): 858-872.(in chinese). DOI:https://10.16058/j.issn.1005-0930.2022.04.006.

Zhang, T., Peng, J., Liang, W., Yang, Y., Liu, Y., 2016. Spatial–temporal patterns of water use efficiency and climate controls in China's Loess Plateau during 2000–2010. Sci. Total Environ. 565, 105–122.

Zhang, J., Tian, H., Shi, H., Zhang, J., Wang, X., Pan, S., Yang, J., 2020. Increased greenhouse gas emissions intensity of major croplands in China: Implications for food security and climate change mitigation. Glob. Chang. Biol. 26 (11), 6116–6133.

Zheng, Z.and Zhang, Y., (2022). Variation in ecosystem water use efficiency and its attribution analysis during 1982–2018 in Qingzang Plateau, China. Chinese J. Plant Ecol., 1: 1-11.(in Chinese). DOI:https://10.17521/cjpe.2021.0187.

Zhong, C., Zolfaghari, A., Hou, D., Goss, G.G., Lanoil, B.D., Gehman, J., Tsang, D.C.W., He, Y., Alessi, D.S., 2021. Comparison of the hydraulic fracturing water cycle in China and North America: a critical review. Environ. Sci. Tech. 55 (11), 7167–7185.

Zhou, Z., Ren, Z., Li, P. et al., (2020). Response of soil moisture content to precipitation under different vegetation coverages. Sci. Soil Water Conserv., 18(6): 62-71.(in Chinese). 10.16843/j.sswc.2020.06.008.

Zhu, Q., Jiang, H., Peng, C., Liu, J., Wei, X., Fang, X., Liu, S., Zhou, G., Yu, S., 2011. Evaluating the effects of future climate change and elevated CO2 on the water use efficiency in terrestrial ecosystems of China. Ecol. Model. 222 (14), 2414–2429.